AN X-BAND FERRITE PHASE SHIFTER

FRANCIS LeROY ROACH

AN X-BAND FERRITE PHASE SHIFTER

by

Francis LeRoy Roach
Lieutenant Commander, U S NAVY

Submitted in partial fulfillment
of the requirements
for the degree of

Master of Science
in
Engineering Electronics

UNITED STATES NAVAL Postgraduate School
Monterey, California

1964

AN X-BAND FERRITE PHASE SHIFTER

by

Francis LeRoy Roach
Lieutenant Commander, US Navy

This work is accepted as fulfilling

the thesis requirements for the degree of

MASTER OF SCIENCE

IN

ENGINEERING ELECTRONICS

from the

United States Naval Postgraduate School

ABSTRACT

Research with ferrites has shown that these materials possess a number of nonreciprocal properties when used in the microwave frequency range. This unusual behavior has led to an increased usage of ferrites in microwave devices.

Extensive experiments conducted at the National Bureau of Standards, Boulder, Colorado, verified the theory and feasability of obtaining precision linear phase shift measurements using ferrites as the control media inside X-Band waveguide. Results of the experiments showed that the ferrites used for phase shift control at X-Band should have the following properties: High mu, low loss tangents, high Curie Temperature, low saturation fields, and high resistivity.

ACKNOWLEDGEMENTS

The writer wishes to thank the members of the NBS Boulder Laboratories for their assistance in carrying out the experimentation of a precision ferrite phase shifter. Particular thanks are extended to Mr. Doyle A. Ellerbruch and Mr. Walter Power, NBS Boulder, and Professor Roy M. Johnson, U. S. Naval Postgraduate School for their cooperation and suggestions in the preparation of this paper.

Table of Contents

Table of Illustrations

Table of Symbols

A	a temperature independent resistivity constant
ATTN	attenuation in decibels (db)
B	flux density
c	velocity of light
db	decibel (unit of attenuation)
$\vec{E}$	vector instantaneous electric field
$\vec{E}_o$	vector normal electric field
e	absolute value of electron charge
Gc	gigocycles
g	Landé g factor of magnetization
$\vec{H}$	vector instantaneous magnetic field
$\vec{H}_o$	vector tangential magnetic field
H_{eff}	effective static magnetic field
H_{DC}	Static magnetic field
H_{rf}	microwave frequency magnetic field
h	an arbitrary propagation constant
J	angular momentum
Kc	kilocycle
k	an arbitrary propagation constant
k_o	a propagation constant for free space
k_b	Boltzmann constant
l	an arbitrary propagation constant
m	mass of the electron
ma	milliamperes
mc	megacycles

M	saturation magnetization
$4\pi M_s$	saturation magnetization
Q	actuation energy
RF	radio frequency
S_{31}	reflectometer taper tune factor
T	absolute temperature
t	time
UHF	ultra high frequency
VSWR	voltage standing wave ratio
x,y,z	three space coordinate system
α	attenuation factor per unit length
β	phase factor per unit length
δ	ferrite slab thickness
γ	gyromagnetic ratio
ϵ_o	dielectric constant of free space
ϵ	dielectric constant of any material
K	tensor permeability factor
K'	tensor permeability loss factor
λ	wavelength
λ_o	wavelength in free space
λ_g	waveguide wavelength
λ_c	cutoff wavelength of waveguide
μ	permeability
$\vec{\vec{\mu}}$	tensor permeability
μ_o	permeability of free space
μ_e	effective permeability

μ_+	permeability with positive circular polarization
μ_-	permeability with negative circular polarization
μ'	real part of permeability tensor
μ''	imaginary part of tensor permeability
ψ	measured phase angle
ρ	resistivity
ω	microwave frequency in megacycles
ω_o	gyromagnetic resonant frequency in megacycles
Γ	general propagation constant
Γ_{2i}	reflectometer short circuit tuning factor
$\frac{\partial}{\partial y}$	symbol for partial derivative

CHAPTER I

INTRODUCTION

I-1. Electromagnetic Propagation Theory

The Propagation of electromagnetic energy in a waveguide (circular or rectangular) is expressed by solutions to Maxwell's Equations in vector form (42)

$$\vec{E} = \vec{E}_o e^{j\omega t} e^{-\Gamma z} \tag{1-1}$$

$$\vec{H} = \vec{H}_o e^{j\omega t} e^{-\Gamma z} \tag{1-2}$$

where $\vec{E}$ and $\vec{H}$ are vector functions of the cross section of the waveguide, $\vec{E}_o$ is normal and $\vec{H}_o$ tangential to the guide surface. The vector can be resolved into rectangular components or circular components. In either case propagation is in the positive z direction. In equations (1) and (2) the symbols are defined as:

$\vec{E}$ = Electric field vector

$\vec{H}$ = Magnetic field vector

ω = angular frequency in radians/sec

t = time

Γ = propagation constant of media inside the waveguide

Since Γ is a function of the media inside the waveguide it can be expressed as

$$\Gamma = \alpha + j\beta \tag{1-3}$$

or

$$\Gamma = j\omega\sqrt{\mu\epsilon} \tag{1-4}$$

where α is the attenuation factor per unit of length, β is the phase factor per unit of length, μ_o and ϵ_o are the permeability and dielectric constants of free space, and μ and ϵ are the permeability and dielectric constants of the medium inside the waveguide and are in general complex. In mks units

$$\mu_o = 4\pi \times 10^{-7} \quad \text{henry/meter}$$

$$\epsilon_o = \frac{1}{36\pi \times 10^{9}} \quad \text{farads/meter}$$

If the medium inside the waveguide is a vacuum, then it is readily seen that $\alpha = 0$ and $\Gamma = j\beta$ or that the electromagnetic energy only experiences a phase shift as it travels down the waveguide.

Even in waveguides filled with air there is some attenuation and phase shift as μ and ϵ are not exactly equal to μ_o and ϵ_o.

If however any material other than air is inserted in the propogation path, α and β become significant and must be considered in solving the boundary value problem and Maxwell's Equations.

From this discussion it would seem possible that phase shift and attenuation in a waveguide can be controlled if the dielectric constant, permeability, or electrical length of the waveguide can be varied. This paper will concern itself more with phase shift problem and will not delve into the attenuation problem except where it is necessary to explain how phase shifting is accomplished with accompanying low attenuation.

I-2. Mechanical and Dielectric Phase Shifters

One way of changing phase in an air filled waveguide would be

to change the electrical length of the waveguide. This can be accomplished, in a rectangular waveguide, by changing the wide dimension of the waveguide.

It has been shown (42) that when electromagnetic energy is propagating in a waveguide filled with air, the guide wavelength (λ_g) is

$$\lambda_g = \frac{\lambda_o}{\sqrt{1 - \left(\frac{\lambda_o}{\lambda_c}\right)^2}} \qquad (1\text{-}5)$$

where λ_o = free space wavelength of the operating frequency

λ_c = free space wavelength of the cut off frequency for waveguide being considered equal to twice the wide dimension.

The cut off wavelength, λ_c, is equal to twice the wide dimension of the rectangular waveguide. Therefore if the wide dimension is varied the guide wavelength (electrical length) will change, causing a phase shift.

This method of phase shifting causes perturbations in the waveguide with resulting attenuation losses and is also very limited in the amount of phase shift that can be achieved. There are also accompanying mechanical difficulties with this system making it unacceptable as a precision phase shift method.

Another method of accomplishing phase shift in a waveguide is to introduce a dielectric material into the path of propagation. The dielectric material used must have no permeability factor and be complex only in ϵ. Thus the real part of ϵ will vary the phase and the imaginary part the attenuation. For dielectric phase shifters a material with a negligible or very small imaginary part is used in order to keep the

attenuation at a small figure.

Placing a dielectric slab with its long dimension in the z direction (rectangular waveguide), the position of the slab in the waveguide will determine the amount of phase shift.

Consider a rectangular waveguide propagating in the TE_{10} mode, as shown

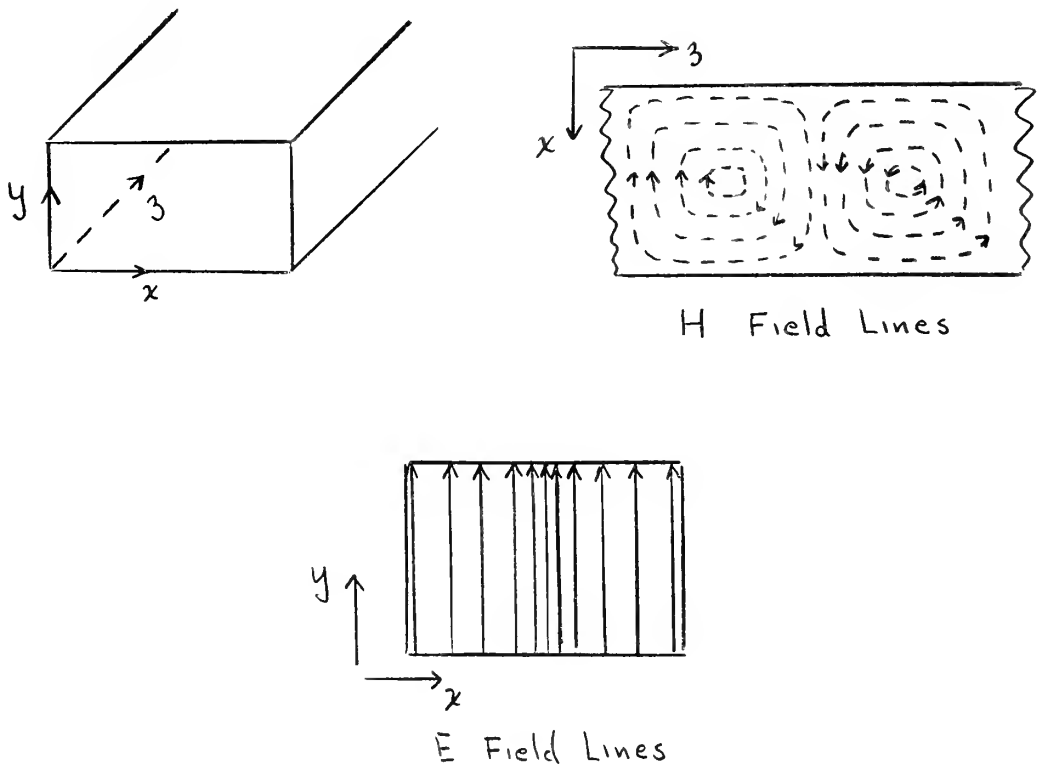

Fig. 1-1. Typical Rectangular Waveguide Fields

The dielectric slab placed at the region of maximum E field will cause maximum phase shift. When along the y waveguide walls minimum phase shift will occur. By making the slab long enough it would be possible to obtain 180° phase shift by varying the position of the slab in the waveguide.

This system requires mechanical linkages which introduce unwanted perturbations and difficulties in obtaining precise position

control.

A. G. Fox (1) developed a somewhat more involved dielectric phase shift device by converting rectangular propagation to cylindrical propagation. Phase shifting is accomplished in the cylindrical section by means of a rotatable dielectric vane. After phase shifting the propagation is converted back to a rectangular system.

The advantage of this system is that phase shifting is continuous through 360^{o}. By very careful construction the attenuation caused by the conversions from rectangular to cylindrical and back to rectangular are kept to a minimum.

The main disadvantage of the mechanical and dielectric phase shift techniques is the limitation of the speed of changing phase due to the mechanical motions involved.

The chief reason for the emphasis on dielectric phase shift devices was the analagous behavior to a parametric amplifier with regards to low noise figure.

1-3. Ferrite Phase Shifters

It wasn't until after Polder (3) showed that the nonreciprocal properties of ferrite loaded microwave devices depended on the tensor properties of the ferrite permeability that any progress was made in using a magnetic material as a means of controlling phase shift.

The tensor representation of the permeability property describes the manner in which the medium responds differently to different senses of propagation.

Since the permeability of the ferrite can be changed by applying an external magnetic field it became possible to develop a phase shifter

with no moving parts and rate of change at electronic speeds.

The next section of this paper will treat the ferrite properties that make phase shifting possible.

CHAPTER II

PROPERTIES OF FERRITES AT MICROWAVE FREQUENCIES

II-1. Brief Historical Sketch of Microwave Ferrite Development

In a sketch by K. J. Button (34), magnetic measurements were made as early as 1890 but usage had been limited up to about one megacycle until 1930 when the need arose for low pass permeability cores above a few megacycles. From 1936-49 effort was devoted on synthesis of polycrystalline materials with suitable magnetic characteristics for rf and microwave frequencies.

In 1948, the Néel (4) theory of ferrimagnetism was announced. In this he postulated that spins of adjacent magnetic atoms are aligned "oppositely", and that the closer the atoms, the stronger the tendency to align oppositely.

Although the basic phenomenon of ferromagnetic spin resonance at microwave frequencies was predicted as early as 1935 by Landau and Lifshitz, a more rigorous quantum mechanical treatment was not provided until 1948-49 by Polder (3).

It wasn't until after Polder's rigorous proof showing the tensor analysis dependence of the nonreciprocal properties of ferrite loaded devices that work really progressed.

Roberts, in 1951, observed the rotation of the E & H fields in a circular waveguide containing a ferrite material. This was also observed by Hogan in 1952-3 (5) and stimulated extensive effort in the field of Faraday rotators.

From an understanding of the Faraday rotator and ferrite property measurements many devices followed: (a) in 1953, a nonreciprocal

phase shifter (8), (b) in 1953, a four point circulator (5), (c) 1956, field displacement isolators (14), (d) 1956, strip line isolators (16), (e) in 1957, predictions for antenna scan techniques (22), and (f) in 1962, power limiters (47).

II-2. Ferrite Properties

The most important properties of ferrites at microwave frequencies are those which are nonreciprocal. A list of some of these properties is:

1) Nonreciprocal Phase Shift
2) Nonreciprocal Displacement
3) Nonreciprocal Rotation (Isolator)
4) Nonreciprocal Birefringence (Modulator)
5) Nonreciprocal Loss (Resonance Isolator)

In addition, there are reciprocal properties under the control of an externally applied magnetic field. Some of these are: Attenuation, phase shift, and modulation.

It is to be remembered that the ferrites used at microwave frequencies are special magnetic crystals and require special preparation. D. L. Fresh (19e) describes the complex problem involved and technique required to make microwave ferrites.

Besides the nonreciprocal and reciprocal properties of ferrites, they can also be classed as having magnetic and non magnetic properties.

II-2a. Magnetic Properties

Magnetic Properties are: Diamagnetism, Paramagnetism, Ferromagnetism, Ferrimagnetism, Antiferrimagnetish, Magnotastatic Energy,

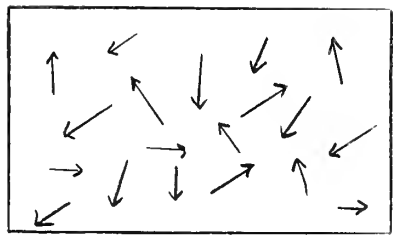

Fig. 2-2. Representation of magnetic dipole orientation in paramagnetic material

Ferromagnetism (Fig. 2-3) is the property by which permanent magnetic dipoles are not oriented at random but show alignment over regions large compared to the atomic volume. These regions (domains) can be aligned by external magnetic field. The domains are random in the material and align only under the influence of an external field.

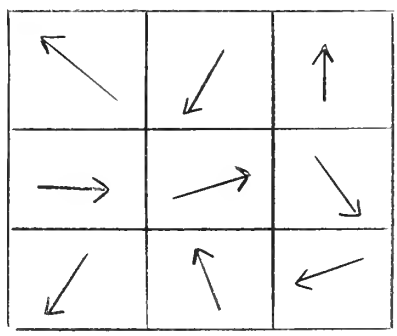

Fig. 2-3. Representation of domain alignment in Ferromagnetic material.

Each of these magnetic properties has associated with it a volume magnetic susceptibility:

1) Diamagnetic materials have a magnetic susceptibility that is negative and of the order of 10^{-5} to 10^{-6} cgs units

2) Paramagnetic materials have a positive magnetic susceptibility of 10^{-4} cgs units

3) Ferromagnetic materials have a positive magnetic susceptibility of 10^{2} to 10^{3} cgs units

Owens (20) and Van Vleck (19a) discuss ferrimagnetism and antiferrimagnetism. Both of these properties were proposed in the Néel Theory of Ferrimagnetism, and are actually special cases of ferromagnetism.

Ferrimagnetism (Fig. 2-4) is that property by which small magnetic moments within a domain align opposite to the large dominant magnetic moments (unequal opposite magnetic moments).

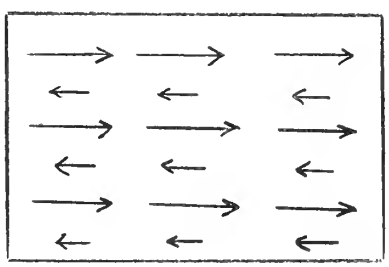

Fig. 2-4. Representation of dipole alignment within a domain of a ferrimagnetic material

Antiferrimagnetism (Fig. 2-5) is like ferrimagnetism except that the magnetic moments are of equal magnitude.

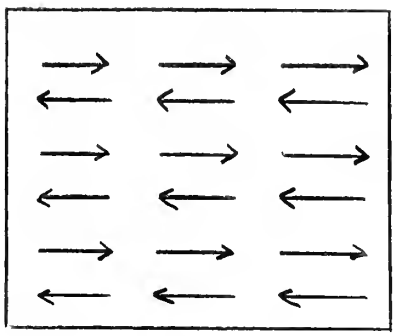

Fig. 2-5. Representation of dipole alignment within a domain of an antiferrimagnetic material

The unit magnetic moment, defined as Bohr Magnetron (20), in ferrites is the spinning electron.

In order to prevent the complete cancellation of the magnetic moments in a domain the ratio of spacing between atoms to the diameter of the electron shell must exceed a minimum of about 1.5 (20).

In a ferrimagnetic material, not in a magnetic field, the magnetic moments tend to align parallel along easy directions of magnetization. The regions of alignment, domains, are interrupted due to impurities, strains, internal fields, imperfections and sample size. The boundary wall between domains is a region of transistions between magnetic moments. The moments at these walls are in unbalance. When an external field is applied, some of these moments will line up with the adjacent domain which is most nearly oriented with the field. This causes the wall between the domains to move thus enlarging the favorable domain (Fig. 2-6). A reversal of the field will cause the wall to move in a reverse direction.

This brief discussion on domain theory describes the magnetic phenomenon in terms of magnetic moments.

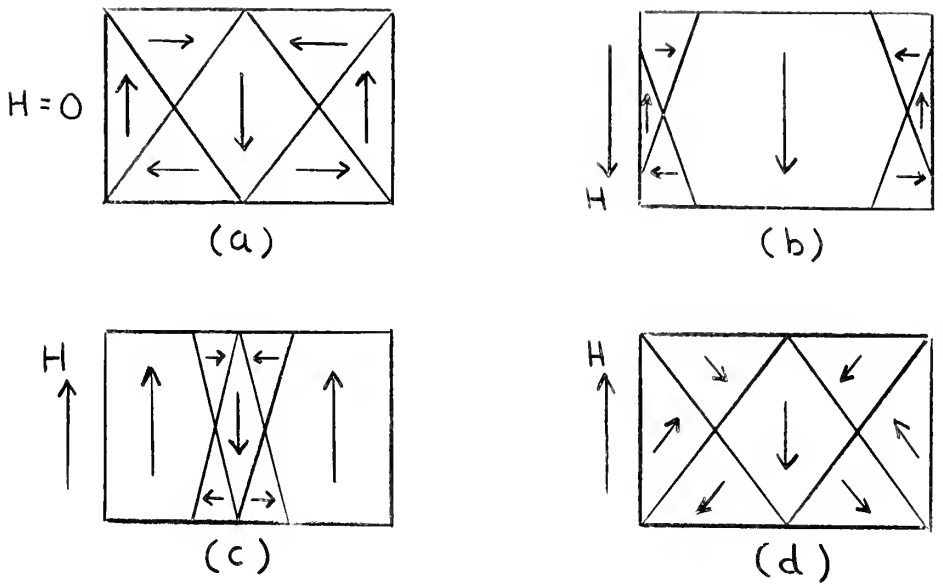

Fig. 2-6. Illustration of domain theory:
(a) No external field, (b) external field applied down, (c) external field applied up, (d) domain structure not effected by H external.

The Magnetostatic Energy, Exchange Energy, Anisotropy Energy, and Magnetoelastic Energy, concepts will be discussed only in general terms, specifics can be obtained from reference (51), section 2-3.

Magnetostatic Energy is associated with the energy on the surface of the material. It is also known as the energy of demagnetization.

Exchange Energy is associated with the boundaries between domains. Since the magnetic moments at the walls cannot be abrupt, there is an energy exchange region. This energy exchange is therefore directly related to the magnetic moment orientation of adjacent domains.

Anisotropy Energy is also closely related to the domain walls. Experimentally it was found that certain ferrites magnetized easier

along certain directions. These were called "easy" axes. The "hard" axes are those which require the largest external field to produce magnetic saturation. Anisotropy energy is defined as the difference between the energy required to magnetize a sample to saturation along the hard direction and that required along the easy axes. One important property to be remembered here is that anisotropy disappears at the Curie Temperature.

Magnetoelastic Energy is associated with the deformity of the magnetic crystal under magnetization.

The Curie Temperature (20) is the temperature above which the material loses its ferromagnetism and reverts to paramagnetism due to thermal agitation. As the Curie Temperature is approached the permeability increases and coercive forces in the crystal reduce. Present day ferrites have a Curie Temperature well above room temperature. The temperature factor is important in working the ferrite.

The best ferrite material is one which exhibits ferrimagnetism, has a high Curie Temperature, low conductivity, high permeability, low coercive forces and a high magnetic moment. Associated with ferrite materials is the saturation moment which is a function of the lattice structure and a "g" factor (Landé g factor (32)) which has been experimentally and theoretically shown to be : g = 2.

II-2b. Non Magnetic Properties

The two significant non magnetic properties of ferrites are resistivity and dielectric constant. These properties are given extensive treatment by L. G. Van Uiter (19d).

By nature, ferrites are semiconductors. Resistivities vary from

5×10^{-3} ohm-cm for magnetite, due to the presence of divalent iron, to well over 10^{11} ohm-cm in certain magnesium and nickel ferrites at room temperatures. Accompanying the high resistivities are low dielectric constants at microwave frequencies. Dielectric constants of the order from 5 - 10 have been observed. However, these same ferrites will have dielectric constants of the order of 10^5 when used at low frequencies.

The exact electrical properties of any given ferrite composition are dependent upon the heat treatment employed in its preparation.

Resistivity of ferrites is also temperature dependent as given by:

$$\rho = A\, e^{Q/k_b T}$$

where ρ is resistivity

A is a temperature independent constant, and depends only on the nature of the material

Q is actuation energy

k_b is Boltzmann constant

T is absolute temperature.

When the natural logarithms of resistivity are plotted vs 1/T, the slopes of the resulting straight line segments represent Q/k for different conduction mechanisms. Fig. 2-7 is such a plot and shows breaks and discontinuities. According to Van Uiter (19d) these breaks are closely related to the Curie temperature and are attributed to crystal structure changes for low temperature breaks, changes in conduction mechanism, and hysteresis effects.

Ferrite	Break Temp	Curie Temp
Mn	335°C	315°C
Cu	480°C	480°C
Ni	595°C	590°C

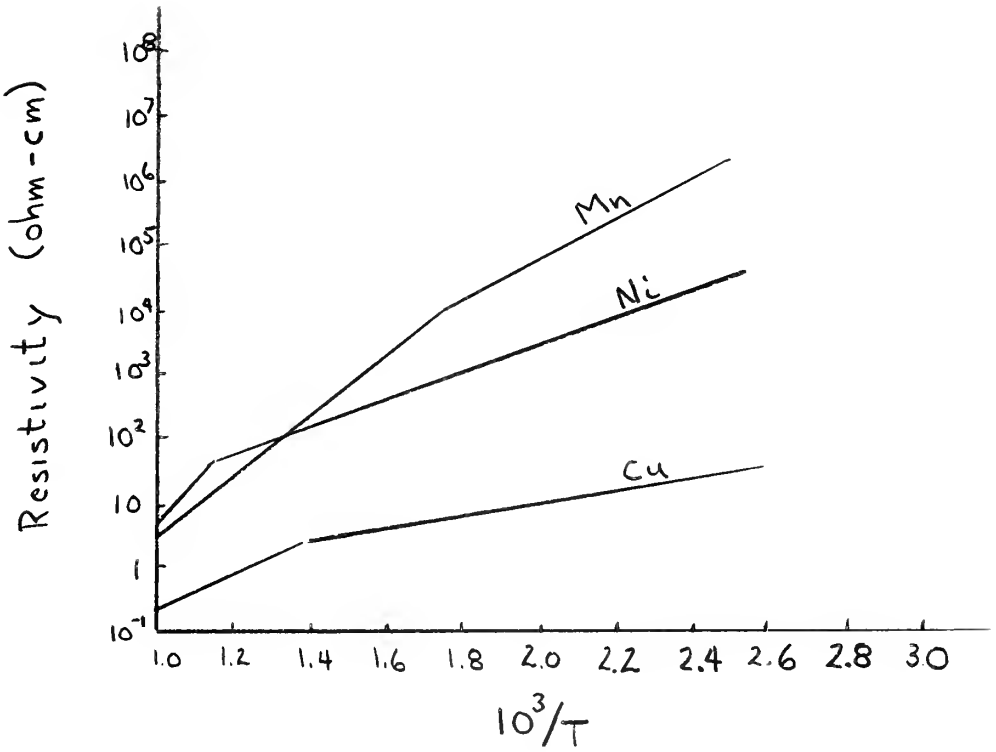

Fig. 2-7. $L_n \rho$ vs $10^3/T$ for various ferrites

II-2c. Loss Mechanisms

There are three methods of approach to the loss characteristics of ferrites: Perturbation Theory, Straight Mathematical Formula Approach, and Experimental Methods.

B. Lax (19g) presents the perturbation theory for measuring loss in microwave ferrite devices. He also makes some comparisons

with actual measurements. P. J. B. Clarricoats (48) presents the mathematical formula approach to losses occurring in ferrites.

C. D. Owens (20) gives a general explanation of the losses that occur in ferrites.

In early magnetic theory, losses were attributed to eddy current and hysteresis. With ferrites and their high resistivity the eddy currents were reduced to such an extent that they became negligible. It was found that there were other losses present which needed examination and explanation. These losses were dielectric properties, domain wall resonance and relaxation, and ferromagnetic resonance. Fig. 2-8 shows how loss varies as a function of internal magnetic field.

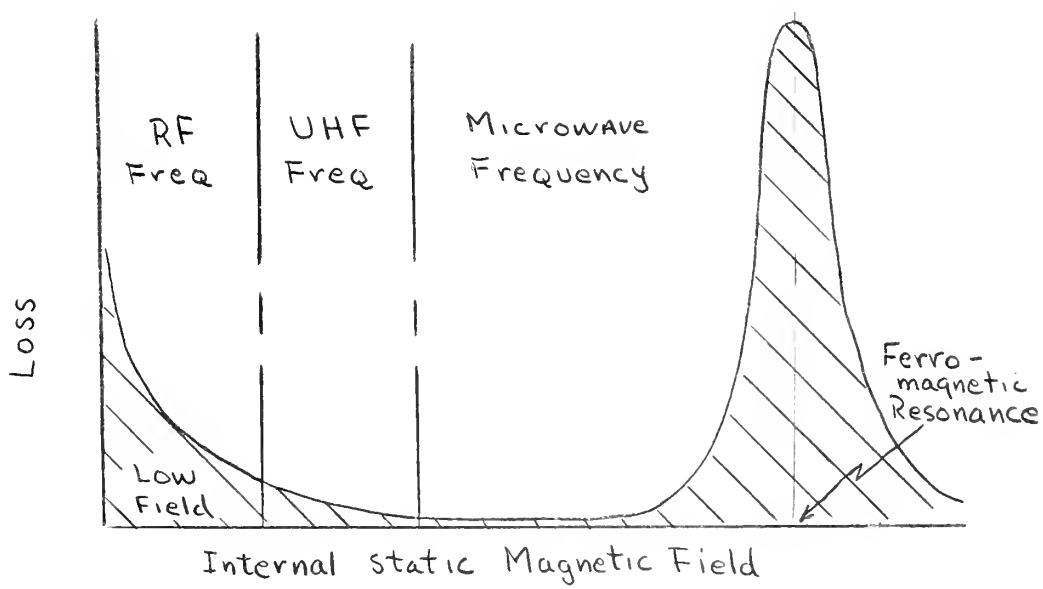

Fig. 2-8. Sketch of losses in a ferrite for various Frequency applications as a function of internal magnetic field.

The low field loss at rf frequency is due to the high dielectric constant of a ferrite at these frequencies. It has been found experimentally that a block of ferrite with a high permeability and

and high dielectric constant at rf frequencies (say about 1 mc) may act as a cavity resonator with a resultant loss in permeability and an increase in core losses.

Other low field losses are those caused by domain wall resonance and/or relaxation. In this instance the domain wall is represented as having inertia, elasticity and dampening; and like an RLC circuit, can resonate at the proper frequency. Large dampening is "relaxation". In ferrites the domain wall resonance can occur between 1 and 100 megacycles depending on the material and shape. Thus at this resonance losses occur.

Hysteresis Loss (45) is the energy loss associated with the magnetic cycle and is proportional to the area enclosed by the β-H curve as in Fig. 2-9.

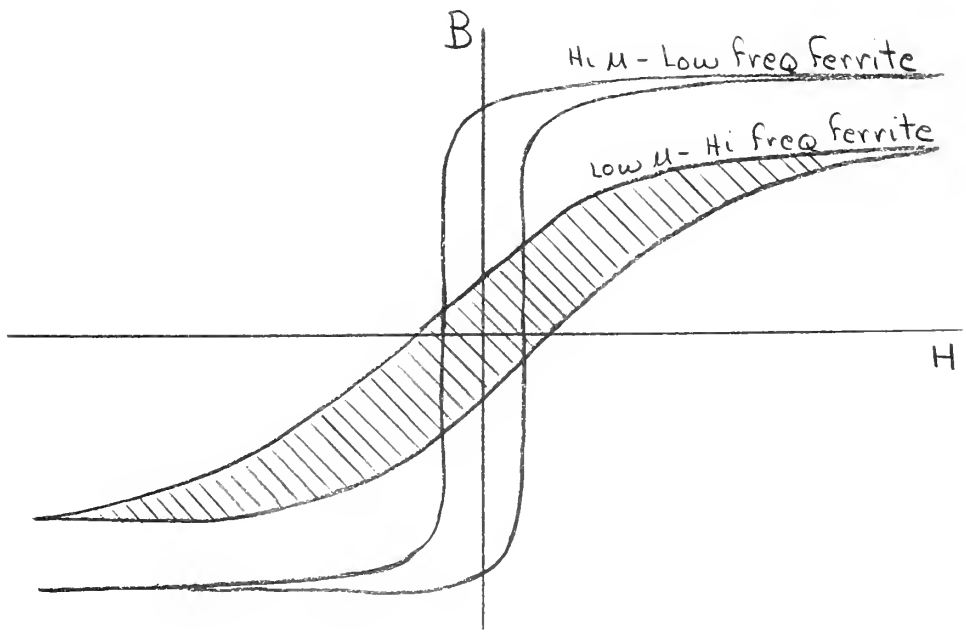

Fig. 2-9. Typical hysteresis curves for ferrites (24)

The hysteresis loop measured under a-c field conditions may differ from that under d-c field conditions due to eddy current losses

widening the loop or the onset of ferromagnetic resonance will cause the shape of the loop to be a function of frequency. Therefore it is desirable to use ferrites with low hysteresis loss over the frequency range of intended usage.

Probably the most important loss mechanism associated with ferrites at microwave frequencies is that of ferromagnetic resonance. This phenomenon comes from the change in permeability with the applied external d-c field which will be discussed in the next section. It has been stated that the ferromagnetic property of magnetic materials comes from the spin of electrons. In ferrites, the spin of cell electrons acting together will produce a net moment for the ferrite. The resonance cause and effects can be explained by looking at a single spinning electron, Fig. 2-10.

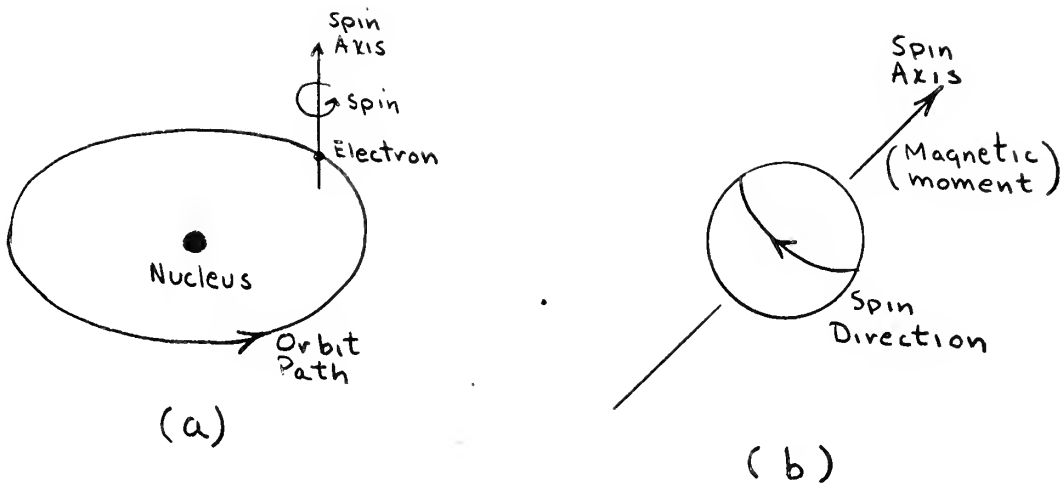

Fig. 2-10. (a) Sketch of spinning electron in orbit

(b) Single spinning electron (enlarged) in magnetic free region

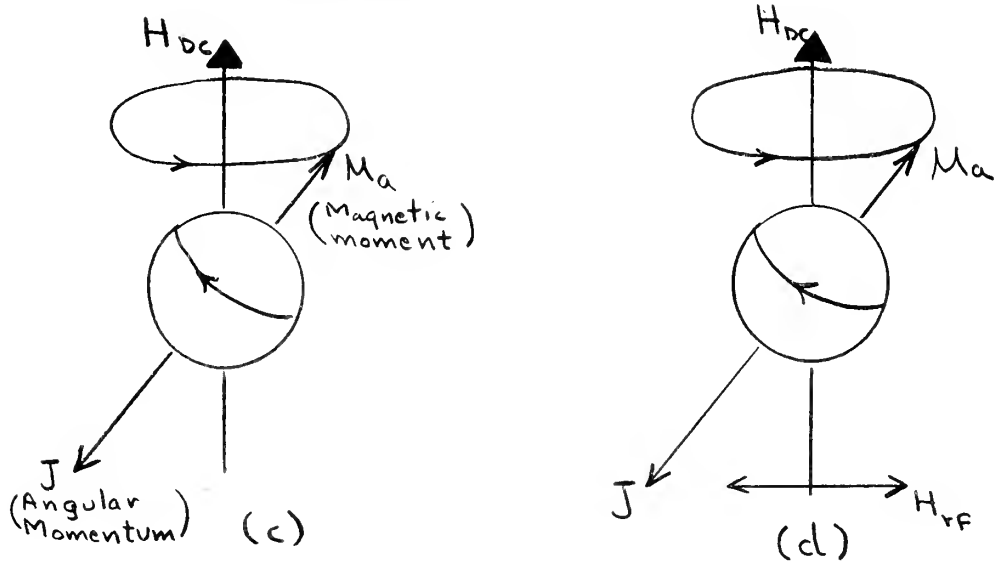

(c) Single spinning electron (enlarged) in the presence of a d-c magnetic field

(d) Same as (c) with an rf field also applied

If an electron is placed in a magnetic field which is not parallel to its magnetic moment (Fig. 2-10c), a torque will be exerted on the electron which will cause it to precess about the applied field with an angular velocity given by

$$\omega_o = \gamma H_{DC} \qquad (2\text{-}1)$$

where

γ is the gyromagnetic ration of $\frac{\text{magnetic moment}}{\text{angular momentum}}$ ($\frac{\text{Mc}}{\text{oersted}}$),

H_{DC} is the applied d-c field (oersted),

ω_o is the gyromagnetic frequency or natural precession frequency

γ is given by

$$\gamma = {}^{ge}/_{2mc} \cong {}^{2.8\,mc}/_{oersted} \qquad (2\text{-}2)$$

where

e is the absolute value of electronic charge

m is the mass of the electron

c is the velocity of light

g is the Landé g factor (32) and is approximately equal to 2.

Thus the precession frequency varies directly as a function of the applied static magnetic field.

Now if an alternating magnetic field (H_{rf}) is applied at right angles to the direction of the static field (H_{DC}), Fig. 2-10d, it is possible to transfer energy from the rf magnetic field to the electron spin. This energy is used to overcome the dampening factor in the precession of the electron about the static field. As the rf magnetic field frequency approaches the precession frequency large amounts of energy are absorbed by the electron spin and the

amplitude of precession will grow. Thus at high frequencies it is possible for a ferrite to act as an attenuator.

The equation of motion for the electron spin is not a simple relationship but is dependent on an analysis of the permeability tensor.

II-2d. Permeability Tensor

Permeability is in general defined as the ratio of flux density to magnetic field intensity.

$$\mu = \frac{B}{H} \tag{2-3}$$

If a ferrite material is subject only to d-c magnetic field the magnetic moment (Magnetization) of the spinning electron will precess about the d-c field and at the same time spiral inward in response to the dampening forces. Thermal agitation keeps the magnetization from completely lining up with the d-c field (41). Now if a ferrite is under the influence of d-c field and a superimposed rf field acting at right angles, the permeability is no longer a linear factor but takes on a tensor form.

Polder (3) showed that a ferromagnetic medium, homogeneously magnetized to saturation is characterized by a permeability tensor given by

$$\vec{B} = \overleftrightarrow{\mu} \cdot \vec{H} \tag{2-4}$$

where $\vec{B}$ and $\vec{H}$ are rf flux density and magnetic field intensity and $\overleftrightarrow{\mu}$ is a tensor of form

$$M = \begin{vmatrix} \mu & -jK & 0 \\ jK & \mu & 0 \\ 0 & 0 & \mu_0 \end{vmatrix} \qquad (2\text{-}5)$$

The components, μ and K, are functions of the static field strength flux density, and magnetization as well as the frequency of the rf field.

The $\overleftrightarrow{\mu}$ tensor is an inherent property of magnetized ferrite media and is applicable to all analyses of ferrite propagation phenomena regardless of the geometry involved (2).

There are many references for the derivation of the permeability tensor (3), (6), (19b), (40), (41), (42), (48), (49), (51), (53). All derivations stem from a discussion of ferromagnetic resonance and which was first explained by Polder (3).

When the tensor permeability is introduced into Maxwell's equations and, a wave equation is derived for propagation in the direction of the applied magnetic field; it has been found that the normal mode solutions are two circularly polarized waves rotating in opposite direction. In this approach the propagation constant for either circular wave contains a simple scalar permeability instead of the tensor required in the general case (7).

In the general case the relationship between b_{rf} and h_{rf} using tensor $\overleftrightarrow{\mu}$ is:

$$b_x = \mu_0 \mu h_x - j\mu_0 K h_y \qquad (2\text{-}6)$$

$$b_y = j\mu_0 K h_x + \mu_0 \mu h_y \qquad (2\text{-}7)$$

$$b_z = \mu_0 h_z \qquad (2\text{-}8)$$

In which H_{DC} is along the positive z axis and propagation is in the positive z direction. The above equations can be represented in tensor form as

$$b_{rf} = \overleftrightarrow{\mu}\, h_{rf} \tag{2-9}$$

where

$$\overleftrightarrow{\mu} = \begin{vmatrix} \mu & -jK & 0 \\ jK & \mu & 0 \\ 0 & 0 & 1 \end{vmatrix} \tag{2-10}$$

$$\mu = \mu_0 + \frac{\gamma M \omega_0}{\omega_0^2 - \omega^2} \tag{2-11}$$

$$K = \frac{\gamma M \omega}{\omega_0^2 - \omega^2} \tag{2-12}$$

$$\omega_0 = \gamma H_{DC} \tag{2-13}$$

in which

$\gamma \triangleq$ gyromagnetic ratio (2.8 Mc/oersted)

$\omega_0 \triangleq$ gyromagnetic resonant frequency

$H_{DC} \triangleq$ DC field in positive direction (oersted)

ω is propagation frequency

μ_0 is permeability of free space

M is saturation magnetization

The scalar expression for permeability can be derived by assuming the ferrite is excited by a clockwise circular polarized field

vector looking along the positive z axis.

Then $$h_y = -jh_x \tag{2-14}$$

and

$$\left.\begin{aligned} b_x &= (\mu - K)h_x \\ b_y &= -j(\mu - K)h_x \end{aligned}\right\} \text{clockwise} \tag{2-15}$$

$$\mu_+ = (\mu - K) = \mu_o - \frac{\gamma M}{\omega_o - \omega} \tag{2-16}$$

For counter clockwise field vector

$$h_y = +jh_x \tag{2-17}$$

$$\left.\begin{aligned} b_x &= (\mu + K)h_x \\ b_y &= +j(\mu + K)h_x \end{aligned}\right\} \text{counter clockwise} \tag{2-18}$$

$$\mu_- = (\mu + K) = \mu_o + \frac{\gamma M}{\omega_o + \omega} \tag{2-19}$$

But μ has both real and imaginary parts, so we let

μ' represent the real part and

μ'' represent the imaginary part.

Figure 2-11 is a plot of μ versus applied magnetic field (H_{DC}) showing both positive circular polarization and negative circular polarization.

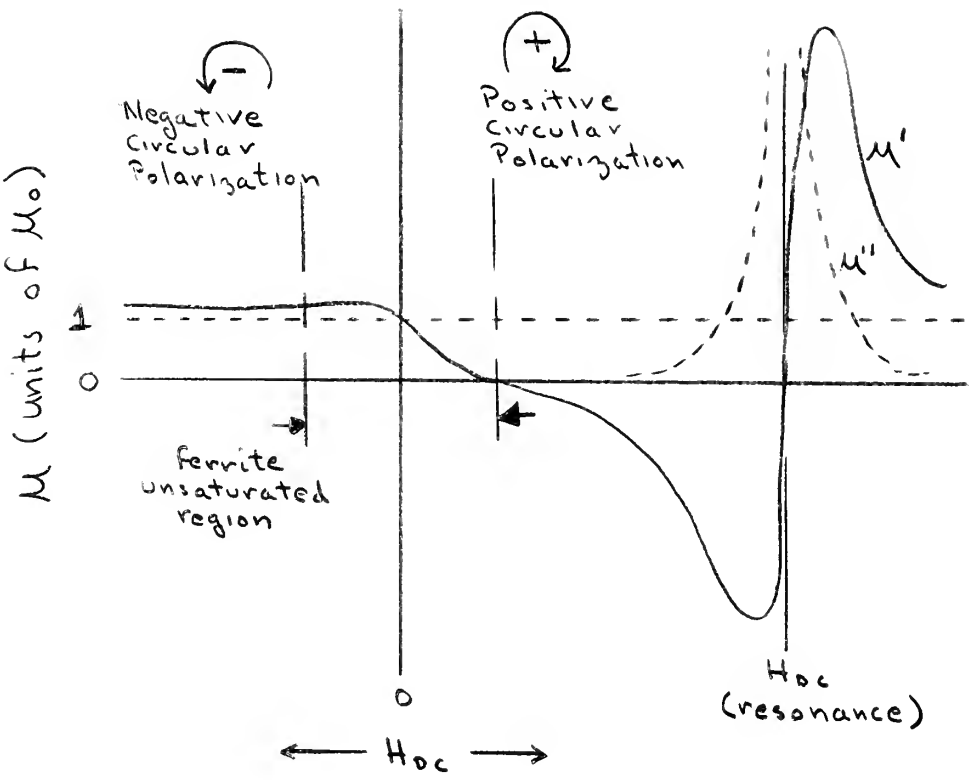

Fig. 2-11. Ferrite permeability for circularly polarized waves as a function of applied DC field.

The foregoing discussion is a derivation of rf permeability which is independent of the shape of the ferrite since it is defined as a ratio of "b" internal and "h" internal (to the ferrite). Since we are more interested in "H" external, it will be convenient to define a μ external as a ratio of b internal to h external. This μ_{ex} will not have a resonance point given by $\omega/|\gamma|$ but rather at a field which is dependent on the ferrite shape. Here a fictitious d-c magnetic field "H effective" is postulated to take into account H_{DC}, rf demagnetization factors and anisotropy field and which will produce the same resonance frequency on an electron in free space as on a ferrite body. Under these conditions Fig. 2-11 can be used

as a universal curve for any shape of body for which an "H effective can be defined".

A relationship between H external, H internal and saturation magnetization for a ferrite material of different shapes is given in reference (54). It is based on the analysis of gyromagnetic resonance conditions and Kittel's equation (2).

CHAPTER III

BOUNDARY VALUE PROBLEM FOR RECTANGULAR WAVEGUIDE CONTAINING FERRITE SLABS

III-1. General

Propagation of electromagnetic waves in a media possessing tensor properties has become a rather common occurrence. Polder presented the theory necessary to understand the way's of the behavior of electromagnetic waves as they passed through the media. Several others (3), (6), (7), (9), (10) have demonstrated the Faraday Rotation effect when microwave energy is passed through a circular waveguide filled with a ferrite material. Soohoo (15) solves the boundary value problem for circular waveguides containing a ferrite rod and clearly demonstrates the difficulty in obtaining physical significance to the equations generated.

Discussion and solution of the wave equations for rectangular waveguides completely filled with ferrite material are presented in (23), (44).

III-2. Transverse Field Problem

The boundary value problem for a transverse field rectangular waveguide containing a ferrite slab was first solved by Button, Lax, Roth (8), (17) and has been reworked by several others (40), (42), (48), (49), (51), (53). It is interesting to note that Chait and Sakiotis (6) in 1953 were conducting experiments with ferrite slabs in a rectangular waveguide in an effort to understand the propagation characteristics.

Since this paper is concerned with transverse field ferrite phase shifters, the boundary value problem will be repeated to demonstrate the practicality of making a precision ferrite phase shift device. The configuration is that of Fig. 3-1.

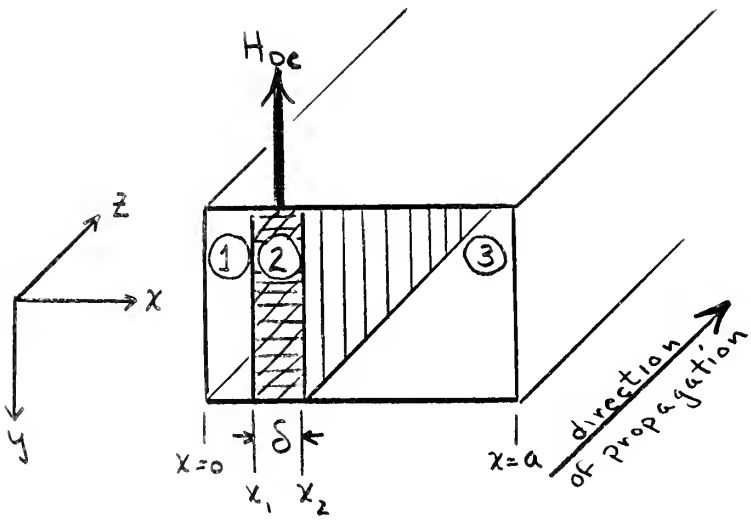

Fig. 3-1. Ferrite loaded waveguide

It is assumed that the ferrite slab is magnetically saturated by the applied d-c magnetic field (H_{DC}) and that region of operation is well below ferromagnetic resonance. Under this condition, the losses will be negligible and the propagation constant will contain only the β term. Further assumptions are that the permittivity ϵ of the ferrite is purely scalar and that the regions in the waveguide not containing the ferrite have $\mu = \mu_o$ and $\epsilon = \epsilon_o$.

Therefore, we state:

a. Region $\left.\begin{matrix} (1)\ \mu = \mu_o \\ (3)\ \epsilon = \epsilon_o \end{matrix}\right\}$ air

b. Region ② $\overleftrightarrow{\mu}$, ϵ (scalar) } ferrite

c. Propagation in positive z direction

d. H_{DC} saturates the ferrite and is the internal field

e. Ferrite is below ferromagnetic resonance

f. $\Gamma = j\beta$

g. $\vec{H}$ (H_x, H_y, H_z) denotes rf magnetic field

$\vec{E}$ (E_x, E_y, E_z) denotes rf electric field

Maxwell's equations for the region containing the ferrite becomes

$$\nabla \times \vec{E}\, e^{j\omega t - \Gamma z} = -j\omega \overleftrightarrow{\mu} \cdot \vec{H}\, e^{j\omega t - \Gamma z} \tag{3-1}$$

$$\nabla \times \vec{H} e^{j\omega t - \Gamma z} = j\omega \epsilon\, \vec{E}\, e^{j\omega t - \Gamma z} \tag{3-2}$$

For simplicity of operation $e^{j\omega t - \Gamma z}$ will not be carried through the rest of the solution but is to be understood throughout.

For H_{DC} in the direction shown

$$\overleftrightarrow{\mu} = \begin{vmatrix} \mu & 0 & -jK \\ 0 & \mu_0 & 0 \\ jK & 0 & \mu \end{vmatrix} \tag{3-3}$$

$$\mu = \mu_0 + \frac{\gamma M \omega_0}{\omega_0^2 - \omega^2} \tag{3-3a}$$

$$K = \frac{\gamma M \omega}{\omega_0^2 - \omega^2} \tag{3-3b}$$

Expanding and separating Maxwell's equation, (3-1) and (3-2) become, with $\partial/\partial y = 0$

$$\Gamma E_y = -j\omega(\mu H_x - j K H_3) \tag{3-4}$$

$$\frac{\partial E_y}{\partial x} = -j\omega(jKH_x + \mu H_3) \tag{3-5}$$

$$-j\omega\epsilon E_y = \Gamma H_x + \frac{\partial H_3}{\partial x} \tag{3-6}$$

$$j\omega\mu_0 H_y = \Gamma E_x + \frac{\partial E_3}{\partial x} \tag{3-7}$$

$$\Gamma H_y = j\omega\epsilon E_x \tag{3-8}$$

$$\frac{\partial H_y}{\partial x} = j\omega\epsilon E_3 \tag{3-9}$$

For TE_{10} Mode equations (3-4), (3-5), (3-6) apply. (3-4) and (3-5) can be combined and solved in terms of H_x and H_z

$$\Gamma E_y + j\frac{K}{\mu}\frac{\partial E_y}{\partial x} = -j\omega\frac{\mu^2 - K^2}{\mu} H_x \tag{3-10}$$

$$-j\frac{K}{\mu}\Gamma E_y + \frac{\partial E_y}{\partial x} = -j\omega\frac{\mu^2 - K^2}{\mu} H_z \tag{3-11}$$

Substituting (3-10) and (3-11) into (3-6) and rearranging, an expression for E_y can be found,

$$\frac{\partial^2 E_y}{\partial x^2} + \left[\Gamma^2 + \omega^2 \epsilon \left(\frac{\mu^2 - K^2}{\mu}\right)\right] E_y = 0 \qquad (3\text{-}12)$$

Let

$$\mu_e = \frac{\mu^2 - K^2}{\mu}$$

then (3-13)

$$\frac{\partial^2 E_y}{\partial x^2} + \left[\Gamma^2 + \omega^2 \epsilon \mu_e\right] E_y = 0$$

This has the same form as

$$\frac{\partial^2 E_y}{\partial x^2} + \left[\Gamma^2 + \omega^2 \epsilon_o \mu_o\right] E_y = 0 \qquad (3\text{-}14)$$

for the field equation in the air filled portion of the waveguide by replacing μ by μ_o and ϵ by ϵ_o and setting K = 0 in equation (3-12).

The general solution for E_y which must vanish at X = 0 and X = a(the guide walls) is

$$\begin{aligned} &\text{Region } 1.\ 0 \le x \le x_1 \ , \ E_y = A \sin hx \\ &\qquad 2.\ x_1 \le x \le x_2 \ , \ E_y = B \sin \ell(x - x_1) + C \sin \ell(x - x_2) \\ &\qquad 3.\ x_2 \le x \le a \ , \ E_y = D \sin h(a - x) \end{aligned} \qquad (3\text{-}15)$$

The solution for region 2 was chosen in order that tangential fields at $X = X_1, X_2$ may be matched. In order for (3-15) to satisfy equation (3-13) the following restrictions are placed on h and ℓ:

$$\Gamma^2 = h^2 - k_o^2 = \ell^2 - k^2 \qquad (3\text{-}16)$$

where

$$k^2 = \omega^2 \mu_e \epsilon$$

$$k_o^2 = \omega^2 \mu_o \epsilon_o$$

.

At $X = X_1, X_2$; E_y must be continuous

$$A \sin h x_1 = - C \sin l \delta \tag{3-17}$$

$$D \sin h (a - x_2) = B \sin l \delta \tag{3-18}$$

where $\delta = X_2 - X_1$, slab thickness.

Also at $X = X_1, X_2$; H_z must be continuous

$$-Ah \cos h x_1 = -\frac{\mu_o}{\mu^2 - K^2}\left[j\Gamma KC \sin l\delta + \mu l C \cos l\delta + \mu l B\right] \tag{3-19}$$

$$-Dh \cos h (a - x_2) = \frac{\mu_o}{\mu^2 - K^2}\left[-j\Gamma KB \sin l\delta + \mu l B \cos l\delta + \mu l C\right] \tag{3-20}$$

The solution for the coefficients A, B, C, D exist only if the determinant of the set of equations vanishes:

$$\begin{vmatrix} \sin h x_1 & 0 & \sin \ell\delta & 0 \\ 0 & -\sin \ell\delta & 0 & \sin h(a-x_2) \\ -h\cosh x_1 & \frac{\mu_0}{\mu^2-K^2}\mu\ell & \frac{\mu}{\mu^2-K^2}\left[\mu\ell\cos\ell\delta + j\Gamma K\sin\ell\delta\right] & 0 \\ 0 & \frac{\mu_0}{\mu^2-K^2}\left[\mu\ell\cos\ell\delta - j\Gamma K\sin\ell\delta\right] & \frac{\mu_0}{\mu^2-K^2}\mu\ell & h\cos h(a-x_2) \end{vmatrix} = 0 \qquad (3\text{-}21)$$

or

$$h\cot h x_1\left[\frac{\mu_0}{\mu_e}\ell\cot\ell\delta - j\frac{\Gamma K\mu_0}{\mu\mu_e}\right] + h\cot h(a-x_2)\left[\frac{\mu_0}{\mu_e}\ell\cot\ell\delta + j\frac{\Gamma K\mu_0}{\mu\mu_e}\right] + h^2\cot h x_1\cot h(a-x_2) + \left(\frac{\mu_0}{\mu_e}\right)^2\left[\frac{\Gamma^2K^2}{\mu^2} - \ell^2\right] = 0 \qquad (3\text{-}22)$$

when $X_1 = 0$, (3-22) reduces to,

$$\frac{\mu_0}{\mu_e}\ell\cot\ell\delta - j\frac{\Gamma K\mu_0}{\mu\mu_e} + h\cot h(a-x_2) = 0 \qquad (3\text{-}23)$$

or when $X_2 = a$, (3-22) becomes,

$$\frac{\mu_0}{\mu_c} \ell \cot \ell\delta + j\frac{\Gamma K \mu_0}{\mu \mu_c} + h \cot h x_1 = 0 \qquad (3\text{-}24)$$

These two characteristic equations are not the same and show that the propagation factor in the positive z direction will differ for ferrite slabs placed along the guide wall at X = 0 or at X = a. Thus nonreciprocal propagation behavior is obtained.

A ferrite slab located at X = a/2, or a waveguide symetrically loaded with the applied field in the same direction for all slabs, will not exhibit a nonreciprocal propagation property.

The solution to equations (3-23) and(3-24) depend on the values of ℓ and h. To solve for these values it is convenient to introduce two new functions:

$$f_1(\beta) = \ell \cot h\delta + h \frac{\mu_c}{\mu_0} \cot h(a - x_2) \qquad (3\text{-}25)$$

$$f_2(\beta) = -\frac{\beta K}{\mu} \qquad (3\text{-}26)$$

It is obvious from these expressions that knowledge of the ferrite parameters: μ, ϵ, K is required, along with δ.

Now, if $f_1(\beta) = f_2(\beta)$, equation (3-23) will be satisfied; and for a given phase constant β, both ℓ and h can be found. If $f_1(\beta) = - f_2(\beta)$, equation (3-24) will be satisfied with same results as just stated.

A plot of the curves of $f_1(\beta) = \pm f_2(\beta)$, and their intersection will determine the propagation constants for the forward and reverse

propagating dominant modes, as shown in Fig. 3-2.

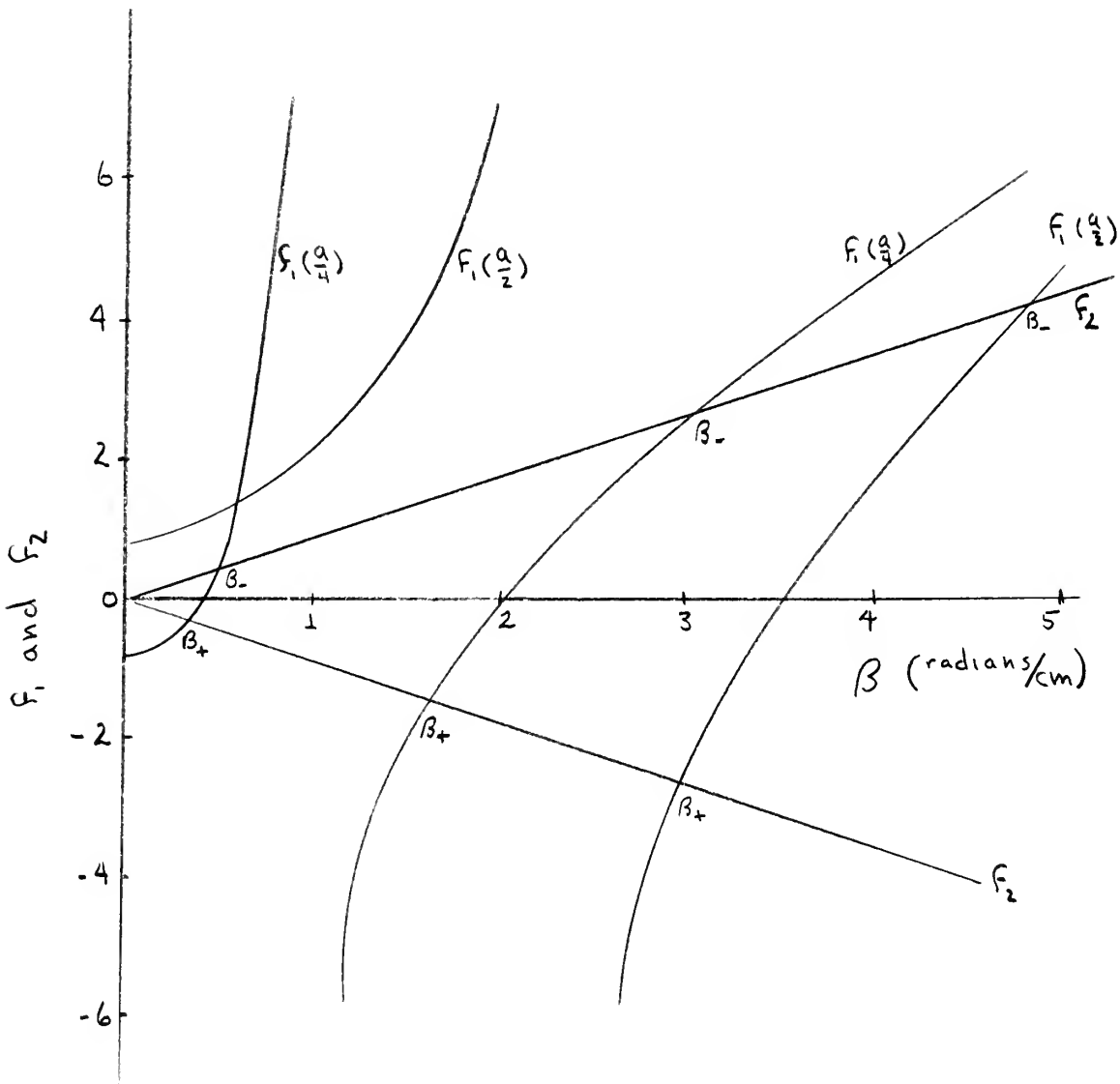

Fig. 3-2. Typical plot of f_1 and f_2 for finding phase constants.
Assumed parameters: $\mu' = \mu = 0.8\mu_0$
$\epsilon = 10\epsilon_0$, $K_0 = 2$, $K = K' = 0.6\mu_0$, $\mu'' = K'' = 0$

According to theory expressed by Collin (42) the modes for $\beta < 3.72$ are the normal perturbed waveguide modes.

Hence it has been demonstrated that the phase constant in a waveguide containing a ferrite is dependent on the intrinsic values of the ferrite as well as its position in the guide and its size. Thus it should be possible to vary the phase of a propagated wave by varying any of these parameters.

CHAPTER IV

X-BAND FERRITE PHASE SHIFTER

IV-1. Longitudinal Field Type

The usual longitudinal X-Band ferrite phase shifter involves conversion of rectangular wave to circular waves and back to rectangular waves. In this manner a circular section of waveguide containing a ferrite rod at the center is used as the phase shift device. This type of device is discussed with its mathematical boundary value problem by Soohoo (15) and is schematically represented in Fig. 4-1.

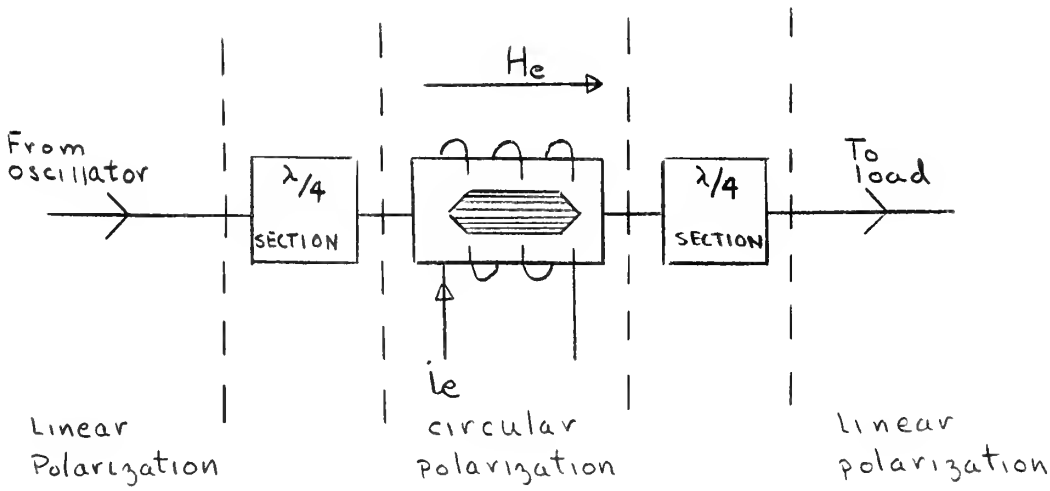

Fig. 4-1. Schematic of longitudinal field phase shifter (i_e DC coil current, H_e DC field applied) (15)

Lax and Button (51) and Barnett (13) also discuss the longitudinal phase shifter. Polydoroff(40) shows pictures of rectangular longitudinal

phase shifters but does not give much information on them. Curves given indicate that they are not very linear with applied field or current. This method also has limited power capability for reasons stated by Clavin (27).

IV-2. Transverse Field Type

The transverse field type phase shifter requires no special conversion from one type waveguide to another. A ferrite slab is inserted in the waveguide and positioned to give the desired propagation features. Magnetic pole pieces are installed so that a uniform magnetic field penetrates the ferrite slab. Phase shifting is accomplished by varying the strength of the magnetic field in the ferrite. This device is schematically represented in Fig. 4-2.

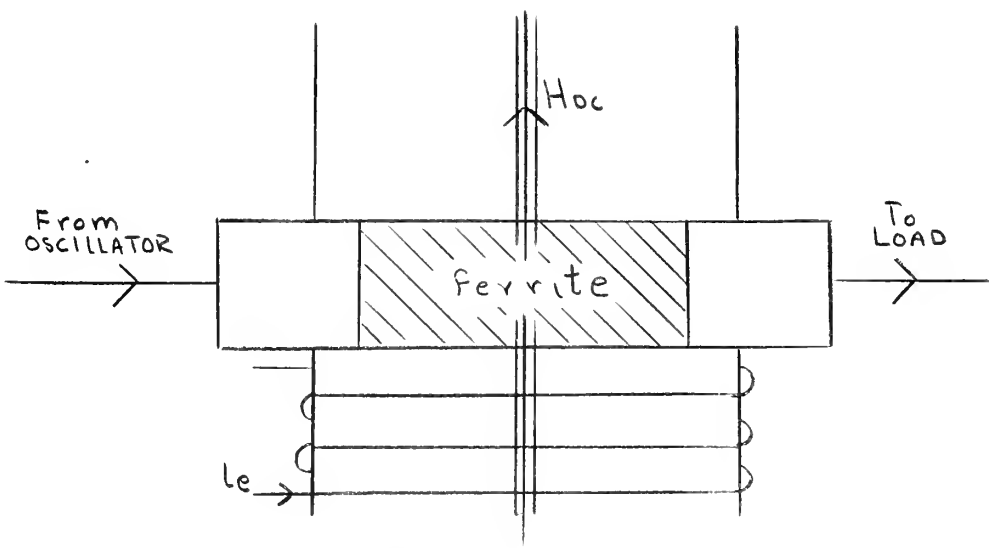

Fig. 4-2. Schematic of transverse field phase shifter

A transverse field ferrite phase shift device should have the following properties (21):

1. Production of an accurate and reproducible phase shift between zero and 360 degrees over an adequate frequency band.

2. Low insertion loss

3. Low VSWR

4. Reciprocity

5. High peak power handling capability

6. Rapid shift to any preset value

7. Low power requirements for remote control operation

8. Operation independent of environmental conditions such as temperature, shock, vibration.

9. Low weight and small volume

The ferrite used in such a device should have:

1. Stability under temperature changes

2. Low loss--constant loss factor over a range of frequencies and temperature

3. High peak power handling capability

4. Ruggedness

5. Homogeneous throughout

6. Require low fields for saturation

The magnet used in such a device should have:

1. Uniform field characteristics at all field strengths

2. Low loss

3. Low heat generation

4. Ruggedness

5. Light weight

6. Very small hysteresis loop

Representative values for ferrite materials and a phase shift device are given in section V-3.

CHAPTER V

EXPERIMENTAL RESULTS AND CONCLUSIONS

V-1. Experimental System

Extensive tests were conducted at the National Bureau of Standards, Boulder, Colorado, using the modulated subcarrier technique of phase shift measurement as a standard. This system was developed at the National Bureau of Standards (37), a sketch of which is presented in figure 5-1. Voltage Standing Wave Ratio (VSWR) and Power Loss were measured using the modified reflectometer technique (55) presented in block diagram in figure 5-2.

Tests were conducted using ferrite material obtained from TRANS-TECH INC, Gaithersburg, Maryland. The dimensions of the actual samples used are given in figure 5-3. The purpose of the tests was to determine which ferrite sample and its position in the waveguide gave the best phase, VSWR, and Loss characteristics. All ferrite slabs were cut from the same ingot in an attempt to maintain the same homogeneous properties.

The electromagnet used was a Varian V-4004 with special pole face pieces to convert the circular field to rectangular. The rectangular pole face was six inches by one-half inch. A graph of the field intensity inside a section of X-Band waveguide placed between the pole faces, with the small dimension of the waveguide as the pole face spacing, is given in figure 5-4.

The following measurements were made:

a. Phase Shift vs Magnet Current

(1) at different frequencies

(2) with different slab thicknesses

(3) with different slab lengths

(4) with different slab positions

(5) and with different slab shapes.

b. VSWR and Power Loss vs Magnet Current

(1) at different frequencies

(2) with different slab thicknesses

(3) with different slab positions

(4) and with different slab shapes.

Since there is a linear relationship between field intensity and magnet current, all results were plotted against magnet current. The range of frequencies used was limited by the frequency range of modulator (8.9-9.4 Gc) used in the measurement system. All graphs presented in this paper are typical results and are mainly centered around the slab with 0.1042 inch thickness. Data was obtained on all slabs and is on file with Mr. D. A. Ellerbruch, National Bureau of Standards, Boulder, Colorado.

V-2 Results

Phase measurements for the various slab thicknesses at the different frequencies used are presented in figures 5-5, 6, 7. The most linear phase change appeared to center around the 0.1042 inch thick slab. Figure 5-8 shows that this slab thickness at a shorter length loses its linearity very rapidly. Figure 5-9 presents the phase measurements of this slab at all three test frequencies. Phase change linearity is also destroyed as the slab is moved away from the waveguide wall, as is shown in figure 5-10. Phase change as a function

of slab shape appears in figure 5-11. Insertion Phase shift was on the order of 3-5°.

Typical curves of Power Loss and VSWR are presented in figures 5-12 and 5-13. Changing the shape of the slab improves the power and VSWR characteristics as shown in figures 5-14 and 5-15 and also as shown in table 5-1.

Table 5-1. VSWR and Power Loss for various ferrite samples with sample along the waveguide wall and reference power set at 1 dbm (10 mω)

Sample Size Thickness	Sample Shape	Freq. (Gc)	VSWR to 225 ma <( )	Power Loss 0-150 ma <( )dbm	Power Loss 150-225 ma > ( )dbm	Insertion Loss <( )dbm
0.0787 inch	Rectangle	8.970	1.6	0.15	0.5	0.2
		9.168	1.5	0.5	0.7	
		9.372	2.4+	2+	0.8	
	Ramp Taper	9.372	1.15	0.1	0.1	
0.0866 inch	Rectangle	8.970	1.6	0.6	0.6	0.2
		9.168	1.5	0.2	0.2	
		9.372	1.8	0.5	0.1	
	Ramp Taper	9.372	1.21	0.2	0.2	
0.1042 inch	Rectangle	8.970	1.9	0.8	0.8	0.5
		9.168	1.6	0.6	0.6	
		9.372	3.6+	10+	0.0	
	Ramp Taper	9.372	1.53	0.2	0.0	
	Diamond Taper	9.372	1.35	0.4	0.3	
0.0787 inch at $x=\frac{7''}{32}$	Rectangle	8.970	7	3.5	3.0	0.2

+ Note: Later measurements showed that these high readings were due to the misplacement of the ferrite sample in the waveguide. Since these same samples were the ones that were shaped to the ramp and diamond taper, it was impossible to rerun these specific tests.

All of the results presented in this study are subject to error in measurement. The Phase measurement error is discussed in references (38) and (39) and, as it applies to this paper, in appendix A. Power and VSWR measurement error is also discussed in appendix A.

Sample calculations using the data provided bythe ferrite manufacturer and the formulae derived in chapters I - IV are presented in appendix B. Curves using this computed data closely follow the ideal curves indicating that a linear ferrite phase shifter is very practical and predictable.

V-3 Conclusions

As a result of the data obtained to substantiate the theory of developing a precision electronic phase shifter, it is the opinion of this writer that such a device is feasible and practicable.

For the ferrite material used in these tests, it appears that a ramp tapered ferrite slab with the dimensions given in figure 5-16, placed in a precision section of waveguide as shown in figure 5-17, with an electromagnet in position as in figure 5-18, should be used. The electromagnet coil current control should be highly regulated and the pole face material should be such as to have a near zero hysteresis loop.

Desireable representative values for ferrite materials to be used at X-Band for phase shifting are:

1. High Curie Temperature, greater than 300^{o}C
2. Low loss, loss tangent should be less than 0.00005
3. Low saturation fields, between 1000 and 2000 gauss

4. Scalar dielectric constant of about 10

5. High resistivity of about 10^{10} ohm/cm

Representative values for a phase shift device at X-Band using ferrites:

1. Low insertion phase shift, less than 5°
2. Low insertion loss, less than 0.5 dbm
3. Low VSWR, less than 1.1
4. Low absorption loss across linear phase shift region, less than 1 dbm
5. Ruggedness and efficient heat sink, to be obtained by using precision waveguide with very thick walls.

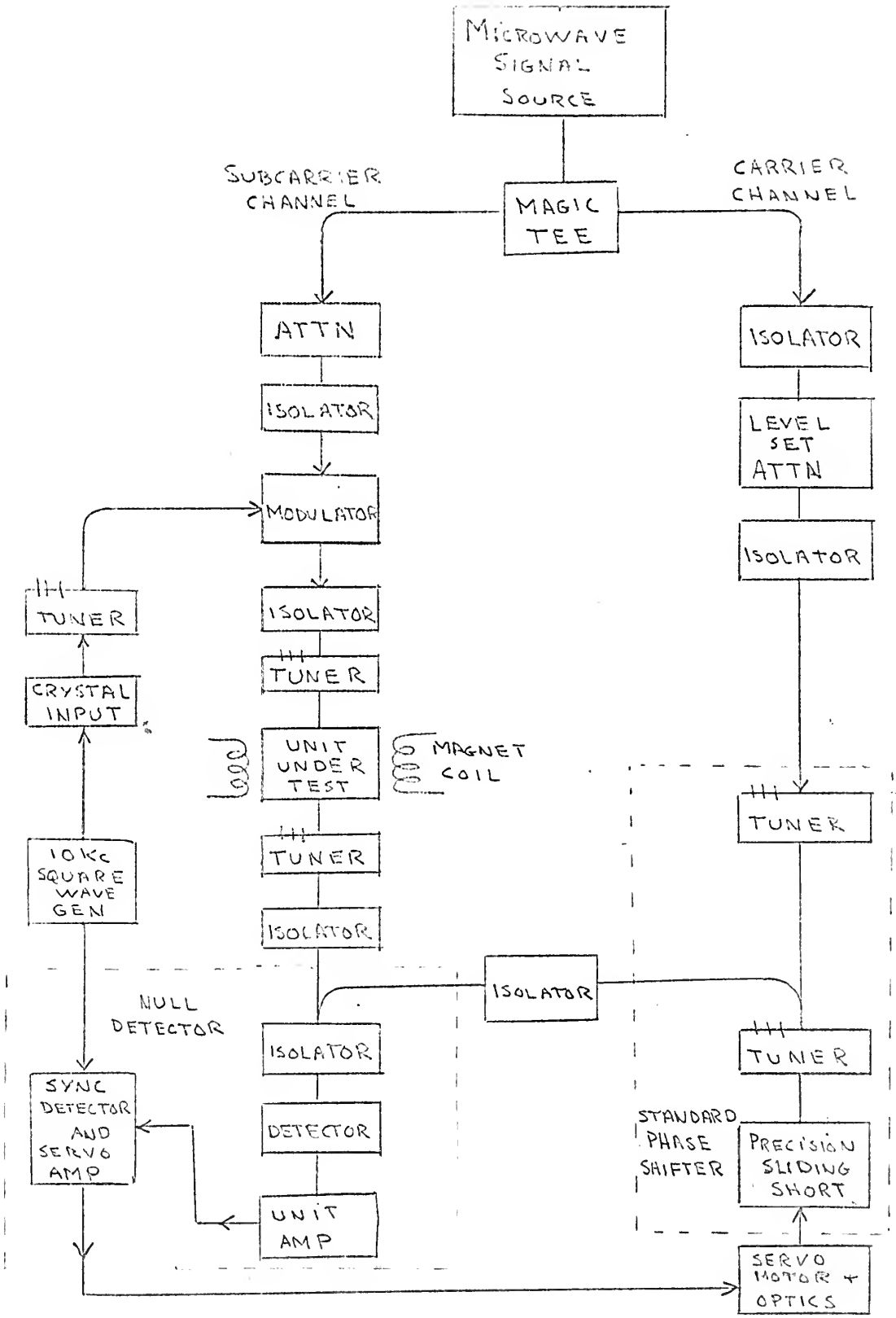

FIG. 5-1. MODULATED SUBCARRIER PHASE SHIFT MEASUREMENT SYSTEM

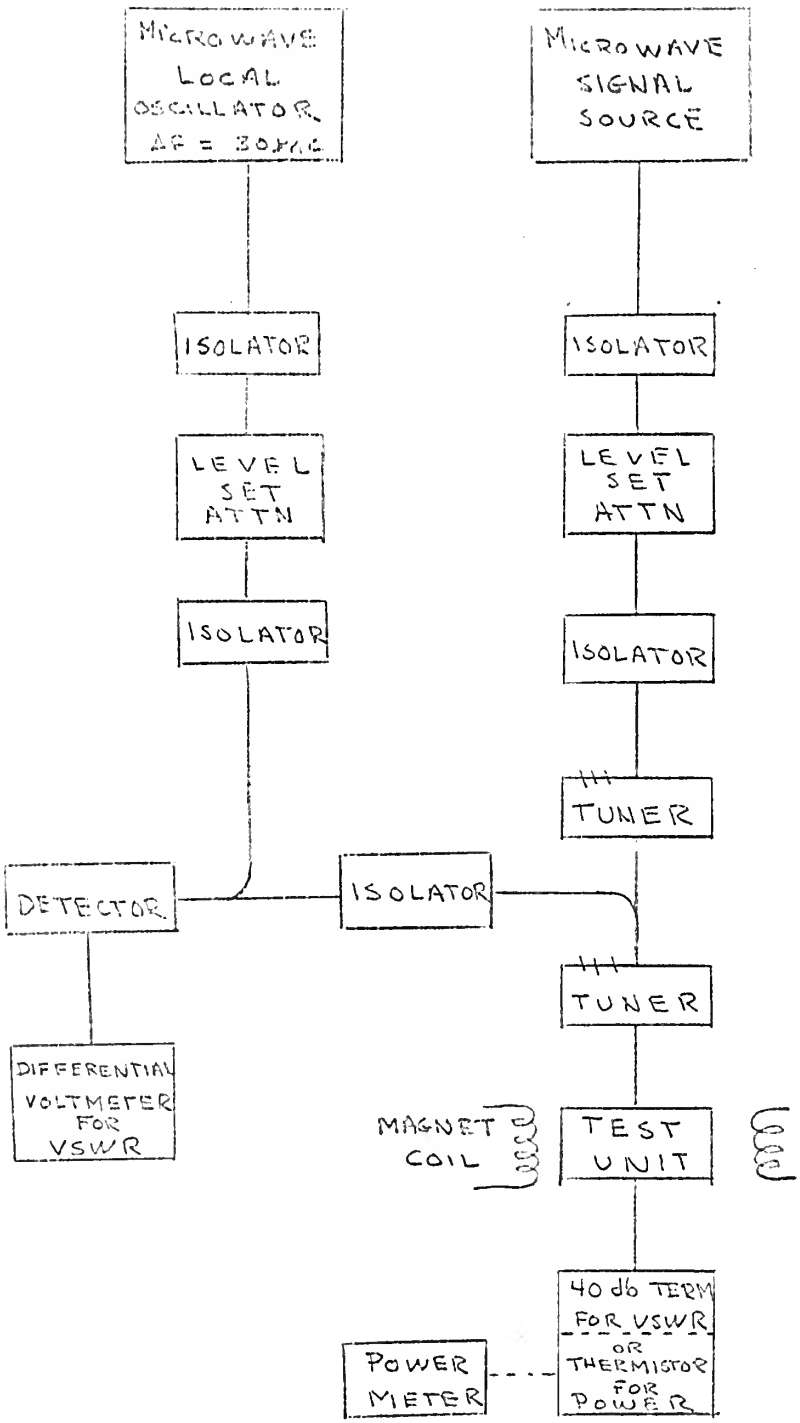

FIG. 5-2. POWER AND VSWR MEASUREMENT SYSTEM

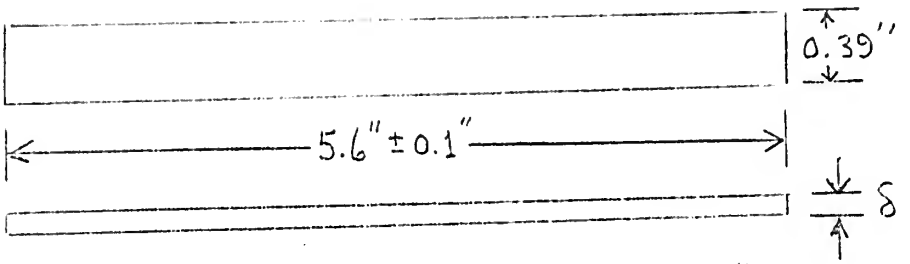

a. RECTANGULAR $\delta = \begin{cases} 0.0545" \\ 0.0787" \\ 0.0866" \\ 0.1042" \\ 0.128" \end{cases}$

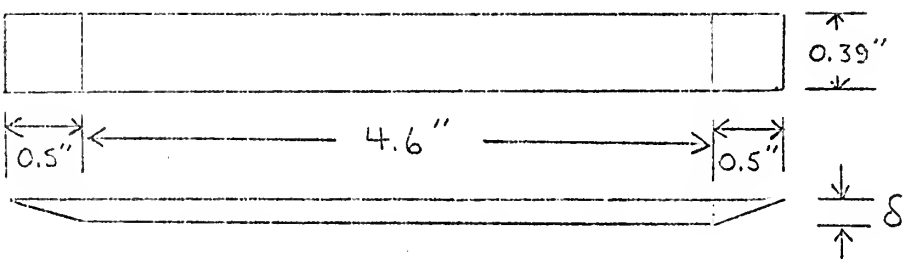

b. RAMP TAPER $\delta = \begin{cases} 0.0787" \\ 0.0866" \\ 0.1042" \end{cases}$

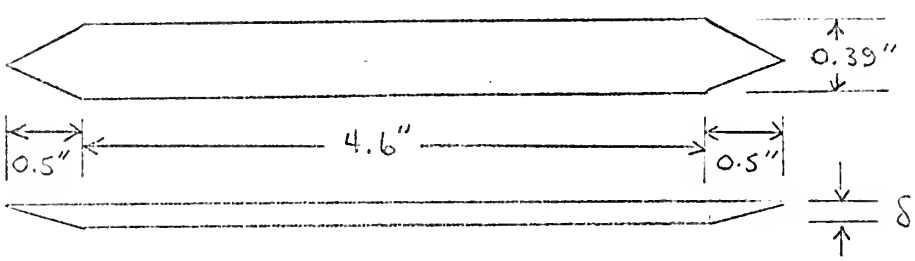

C DIAMOND TAPER $\delta = 0.1042"$

FIG. 5-3 FERRITE SLAB DIMENSIONS

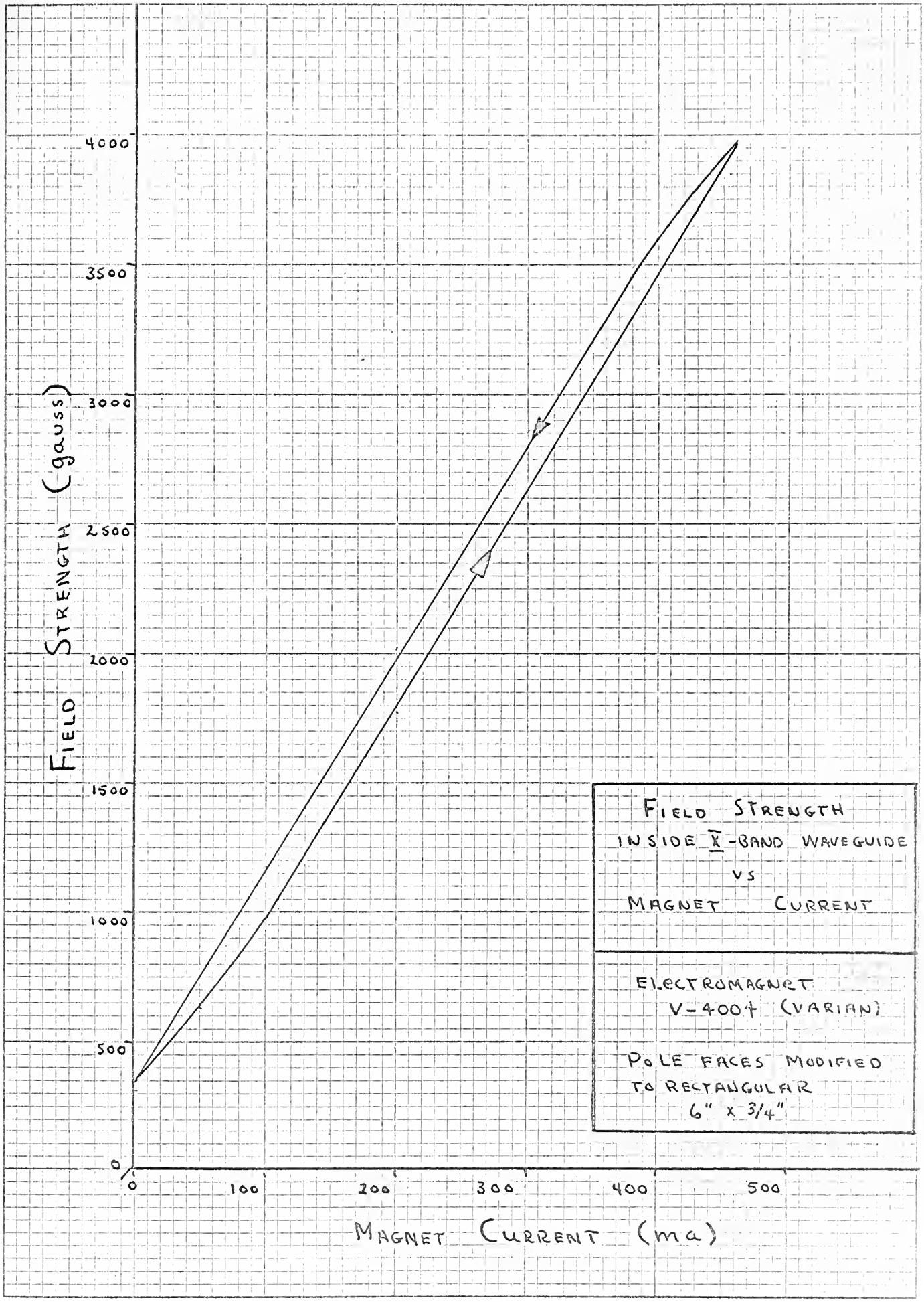
4000
3500
3000
2500
2000
1500
1000
500
0
FIELD STRENGTH (gauss)
0
100
200
300
400
500
MAGNET CURRENT (ma)
FIELD STRENGTH
INSIDE X-BAND WAVEGUIDE
VS
MAGNET CURRENT
ELECTROMAGNET
V-4004 (VARIAN)
POLE FACES MODIFIED
TO RECTANGULAR
6" x 3/4"

FIG. 5-4

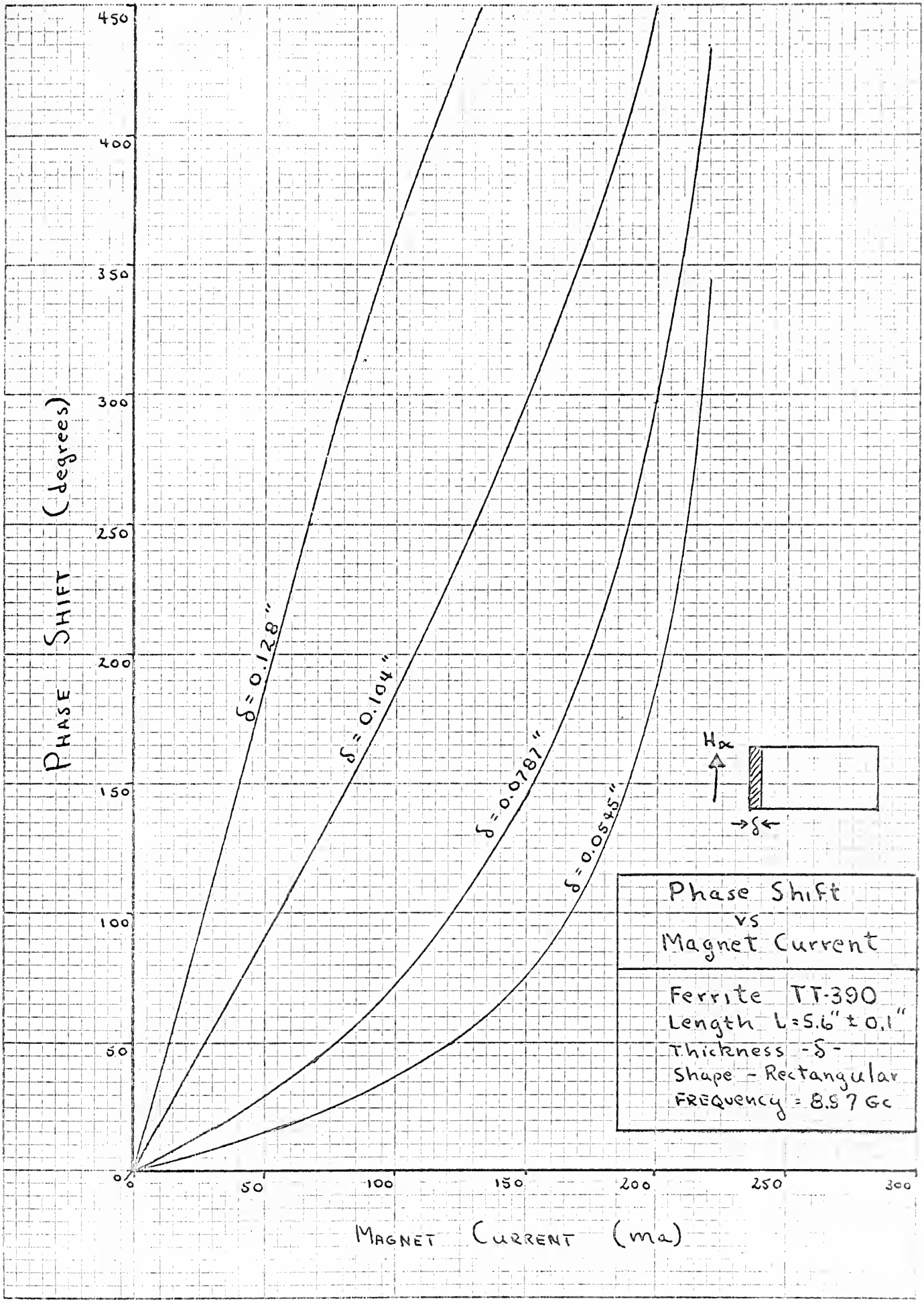
PHASE SHIFT (degrees)
450
400
350
300
250
200
150
100
50
0
0
50
100
150
200
250
300
MAGNET CURRENT (ma)
δ = 0.128"
δ = 0.104"
δ = 0.0781"
δ = 0.0545"
Hα
δ
Phase Shift
vs
Magnet Current
Ferrite TT-390
Length L = 5.6" ± 0.1"
Thickness -δ-
Shape - Rectangular
FREQUENCY = 8.57 Gc

FIG. 5-5

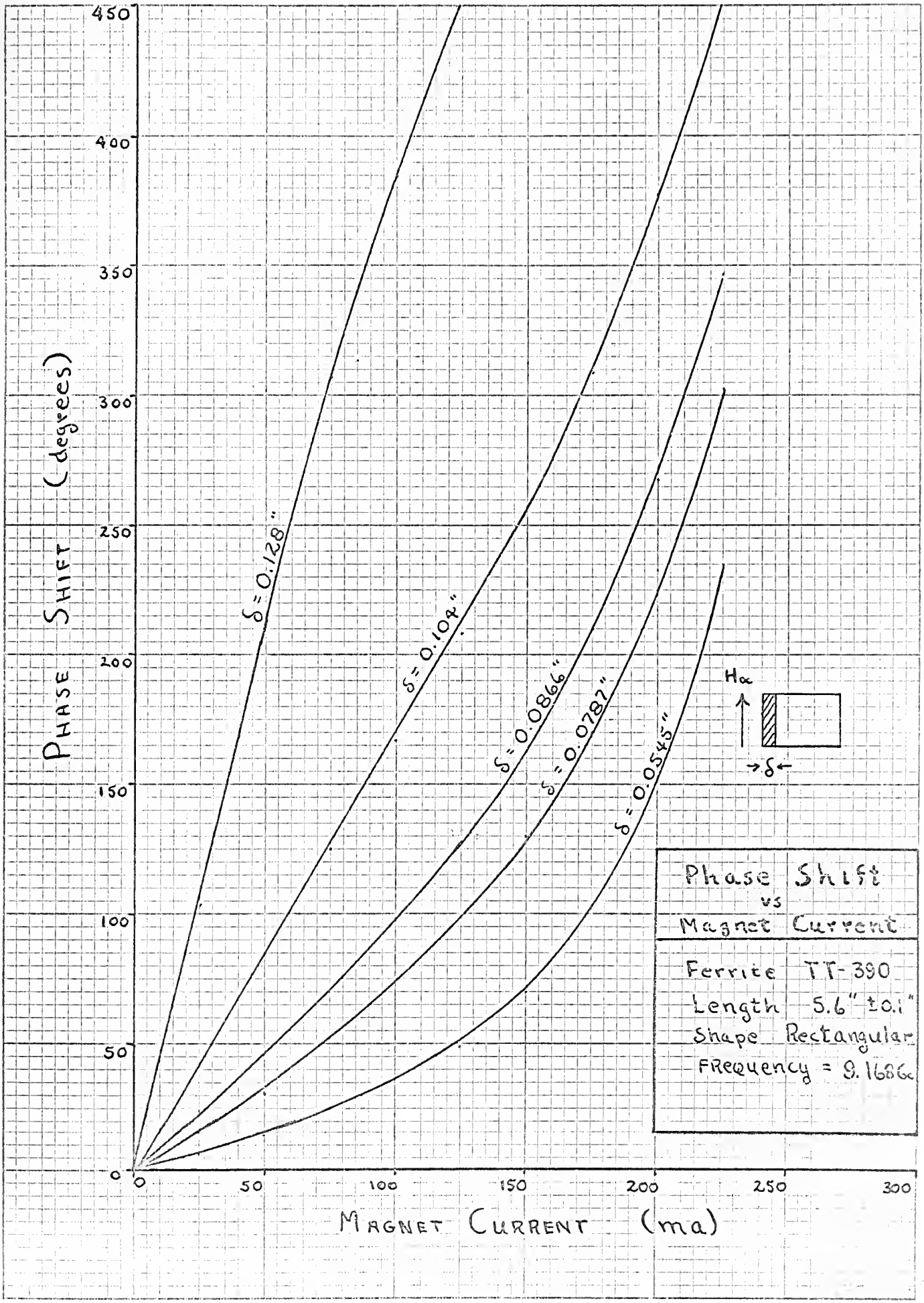
450
400
350
300
250
200
150
100
50
0
PHASE SHIFT (degrees)
δ = 0.128"
δ = 0.104"
δ = 0.0866"
δ = 0.0787"
δ = 0.0545"
Hα
→δ←
Phase Shift
vs
Magnet Current
Ferrite TT-390
Length 5.6" ±0.1"
Shape Rectangular
Frequency = 9.1686
0
50
100
150
200
250
300
MAGNET CURRENT (ma)

FIG 5-6

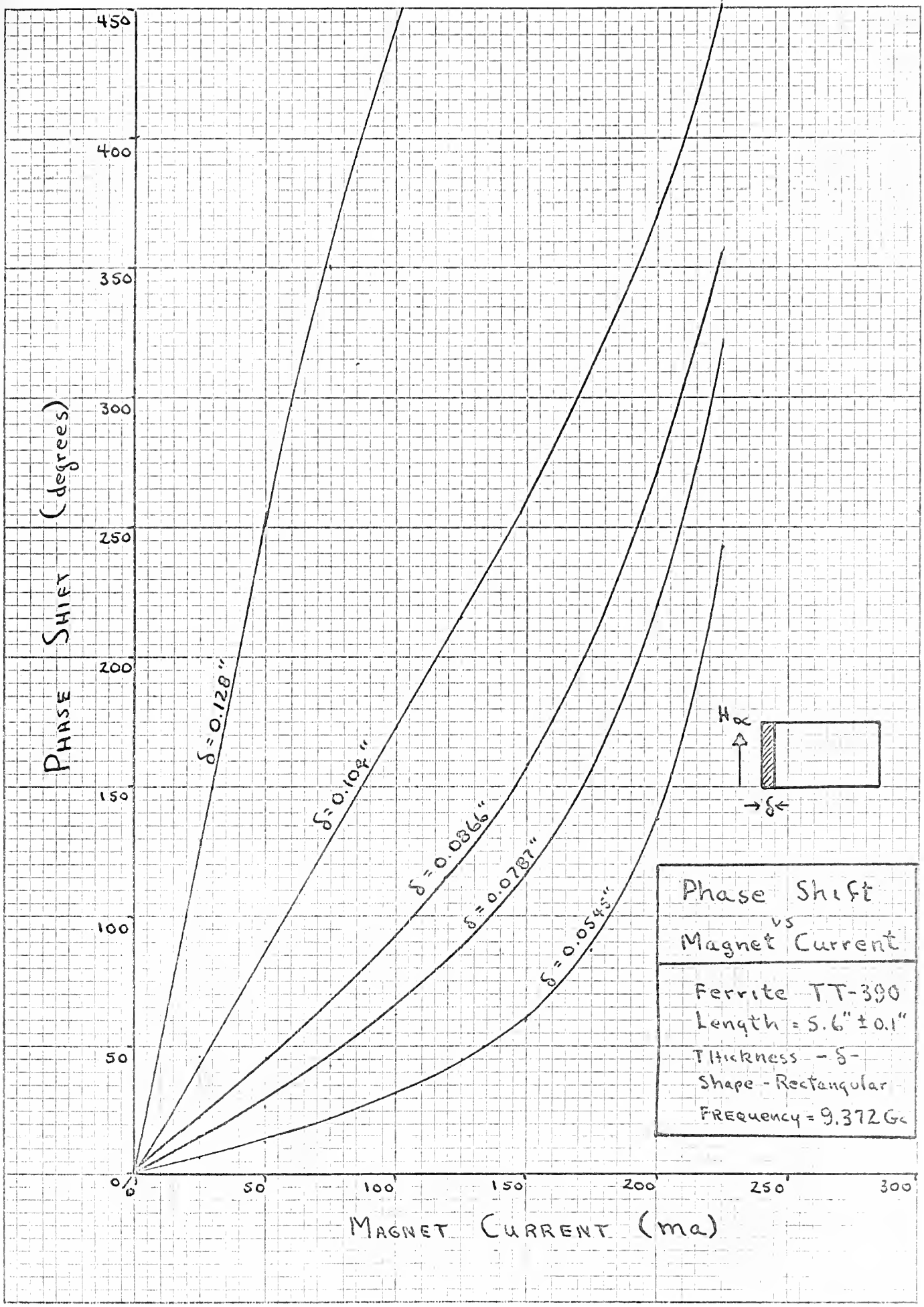
450
400
350
300
250
200
150
100
50
0
PHASE SHIFT (degrees)
δ = 0.128"
δ = 0.102"
δ = 0.0866"
δ = 0.0787"
δ = 0.0545"
H∝
→δ←
Phase Shift
Magnet vs Current
Ferrite TT-390
Length = 5.6" ± 0.1"
Thickness - δ -
Shape - Rectangular
FREQUENCY = 9.372 Gc
0
50
100
150
200
250
300
MAGNET CURRENT (ma)

FIG. 5-7

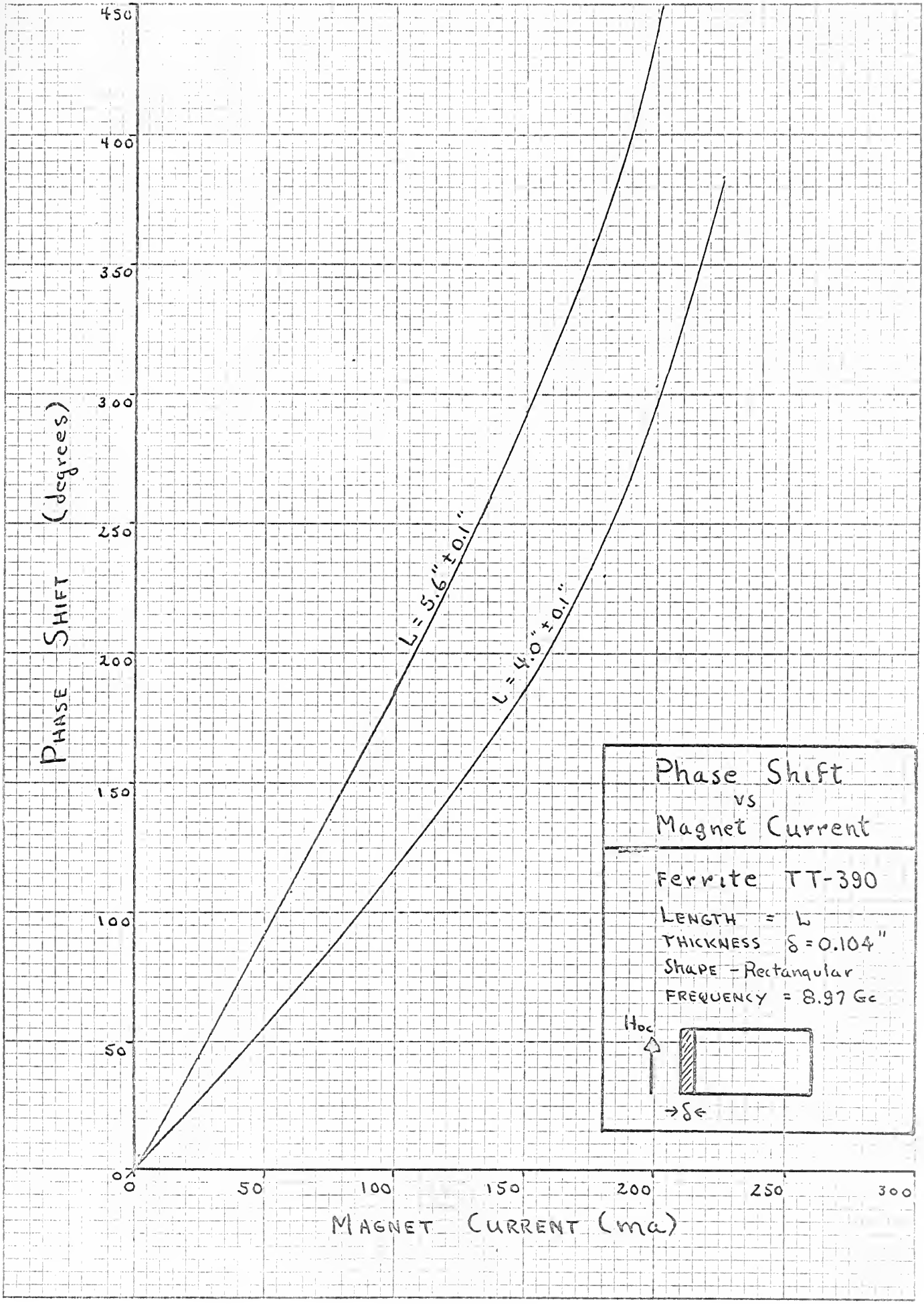
Phase Shift (degrees)
450
400
350
300
250
200
150
100
50
0
0
50
100
150
200
250
300
Magnet Current (ma)
L = 5.6" ± 0.1"
L = 4.0" ± 0.1"
Phase Shift
vs
Magnet Current
Ferrite TT-390
Length = L
Thickness δ = 0.104"
Shape - Rectangular
Frequency = 8.97 Gc
Hoc
δ

FIG. 5-8

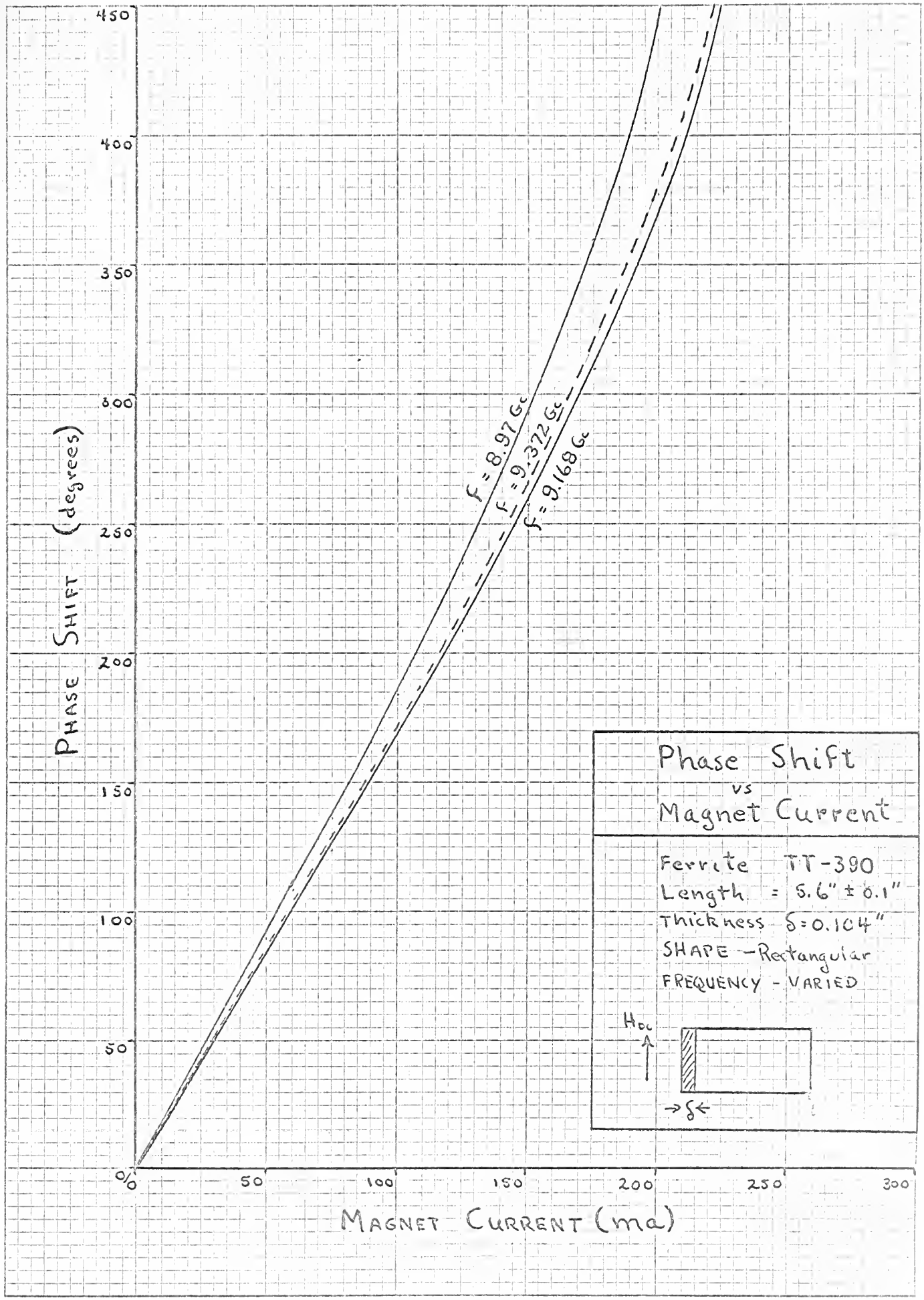
450
400
350
300
250
200
150
100
50
0/0
PHASE SHIFT (degrees)
50
100
150
200
250
300
MAGNET CURRENT (ma)
f = 8.97 Gc
f = 9.372 Gc
f = 9.168 Gc
Phase Shift
vs
Magnet Current
Ferrite TT-390
Length = 5.6" ± 0.1"
Thickness δ = 0.104"
SHAPE - Rectangular
FREQUENCY - VARIED
H_DC
δ

FIG. 5-9

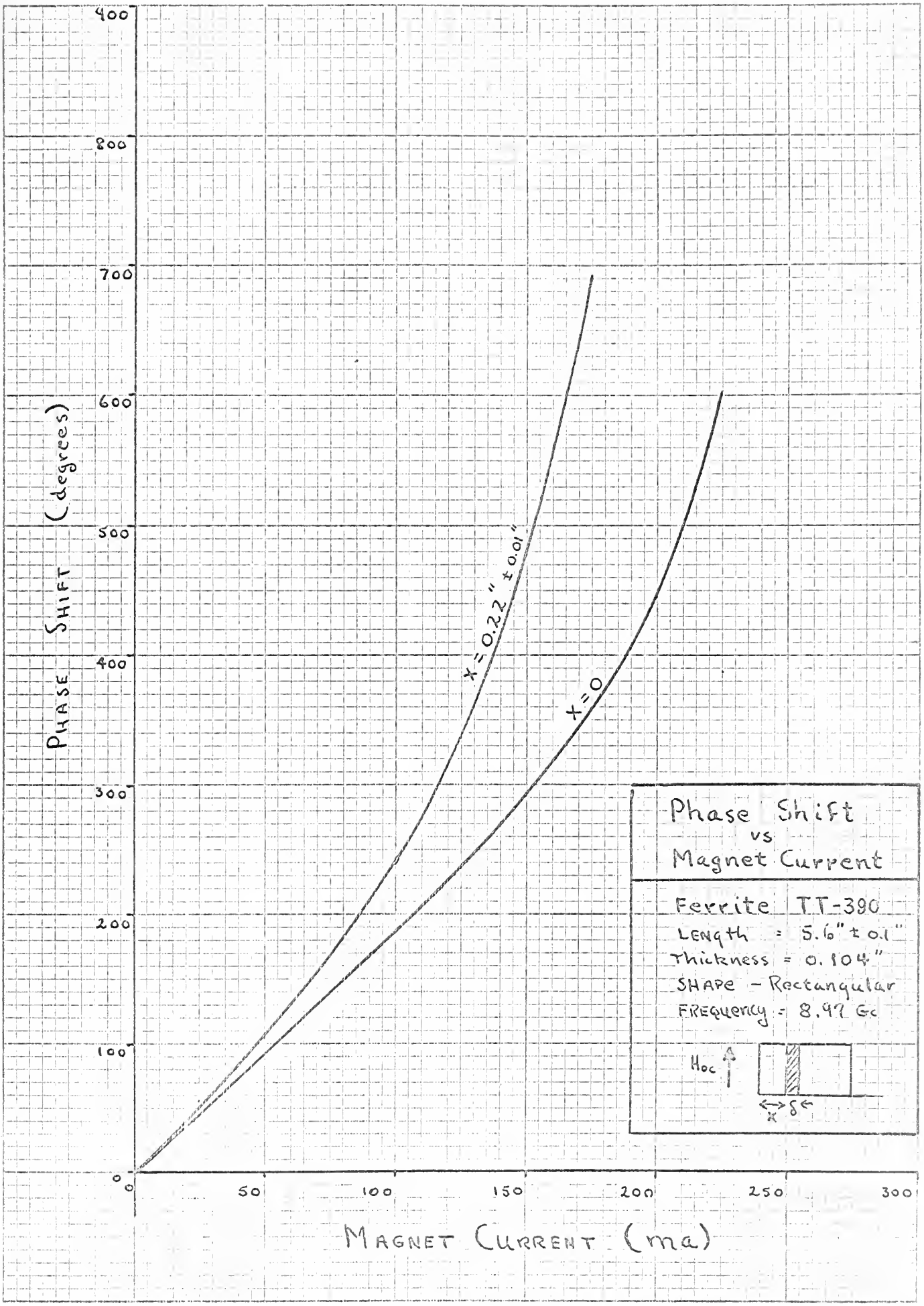
400
800
700
600
500
400
300
200
100
0
PHASE SHIFT (degrees)
x = 0.22" ± 0.01"
x = 0
Phase Shift
vs
Magnet Current
Ferrite TT-390
LENGTH = 5.6" ± 0.1"
Thickness = 0.104"
SHAPE - Rectangular
FREQUENCY = 8.97 Gc
Hoc
δ
0
50
100
150
200
250
300
MAGNET CURRENT (ma)

FIG. 5-10

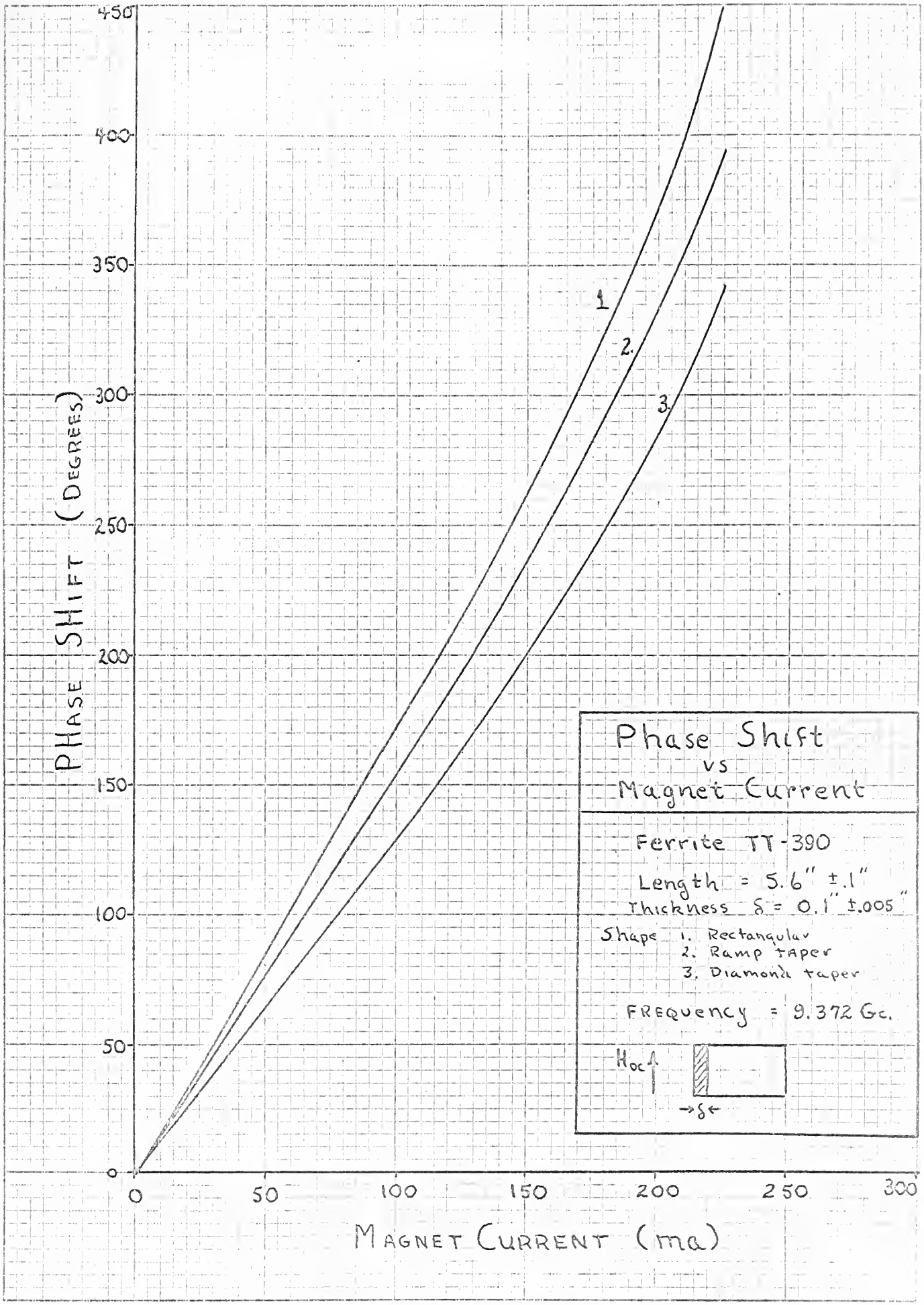
450
400
350
300
250
200
150
100
50
0
PHASE SHIFT (DEGREES)
0
50
100
150
200
250
300
MAGNET CURRENT (ma)
1
2
3
Phase Shift
vs
Magnet Current
Ferrite TT-390
Length = 5.6" ±.1"
Thickness δ = 0.1" ±.005"
Shape 1. Rectangular
2. Ramp taper
3. Diamond taper
FREQUENCY = 9.372 Gc.
Hoc
δ

FIG. 5-11

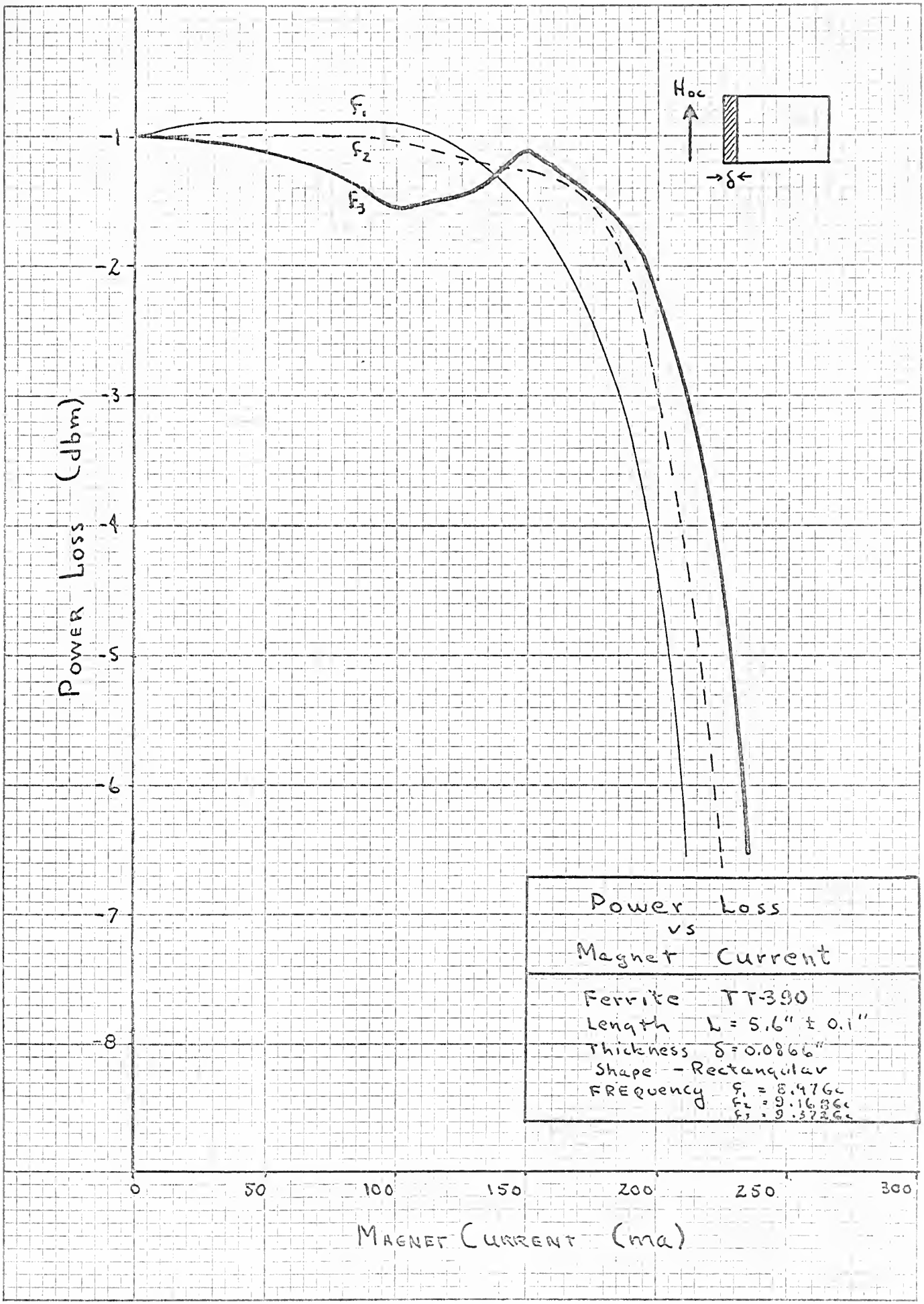
f_1
f_2
f_3
H_{DC}
δ
-1
-2
-3
-4
-5
-6
-7
-8
Power Loss (dbm)
0
50
100
150
200
250
300
Magnet Current (ma)
Power Loss
vs
Magnet Current
Ferrite TT-390
Length L = 5.6" ± 0.1"
Thickness δ = 0.0866"
Shape - Rectangular
FREQUENCY f_1 = 8.47Gc
f_2 = 9.16Gc
f_3 = 9.37Gc

FIG. 5-12

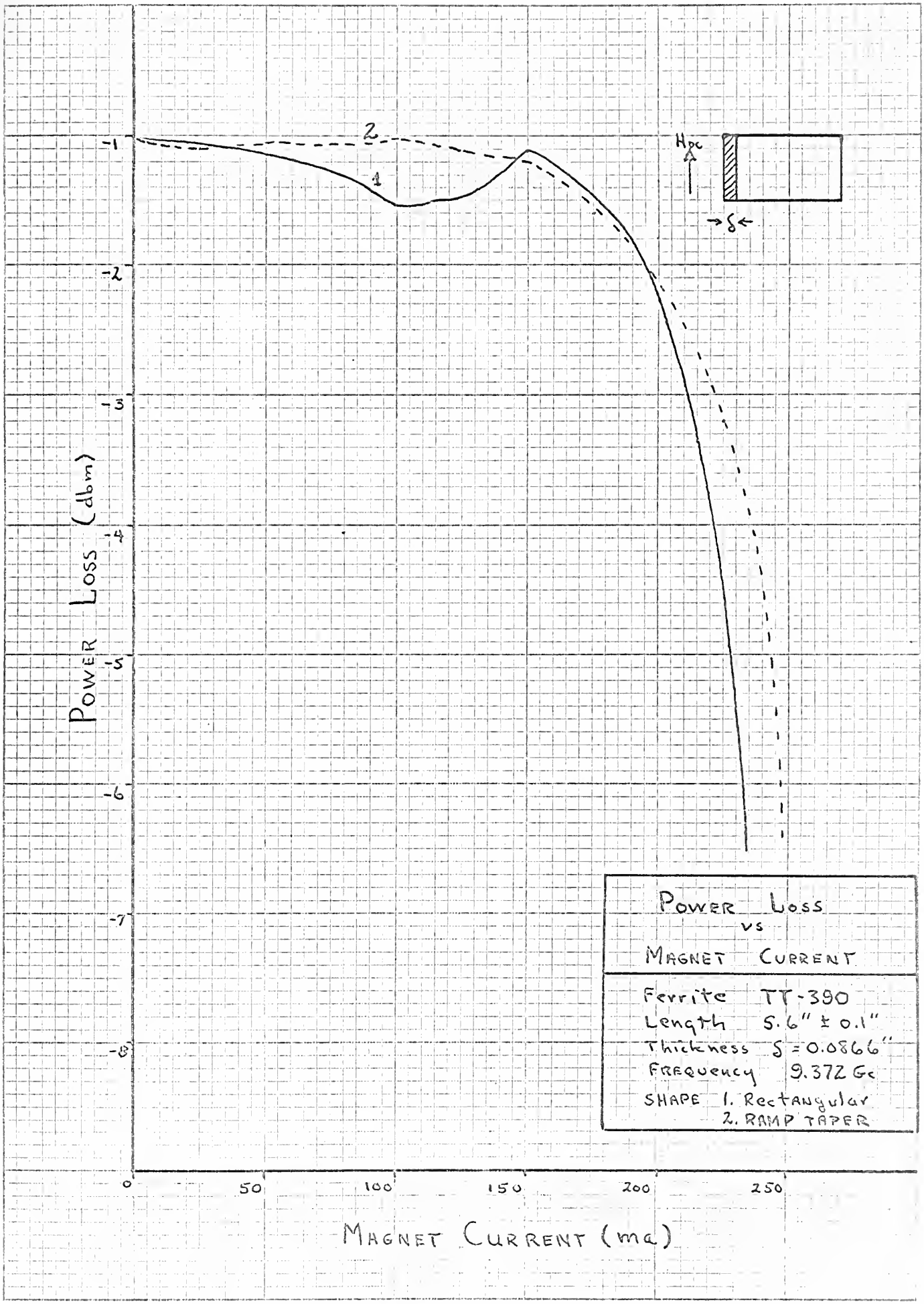
2
1
H_{DC}
δ
-1
-2
-3
-4
-5
-6
-7
-8
Power Loss (dbm)
0
50
100
150
200
250
Magnet Current (ma)
Power Loss
vs
Magnet Current
Ferrite TT-390
Length 5.6" ± 0.1"
Thickness δ = 0.0866"
Frequency 9.372 Gc
SHAPE 1. Rectangular
2. RAMP TAPER

Fig. 5-13

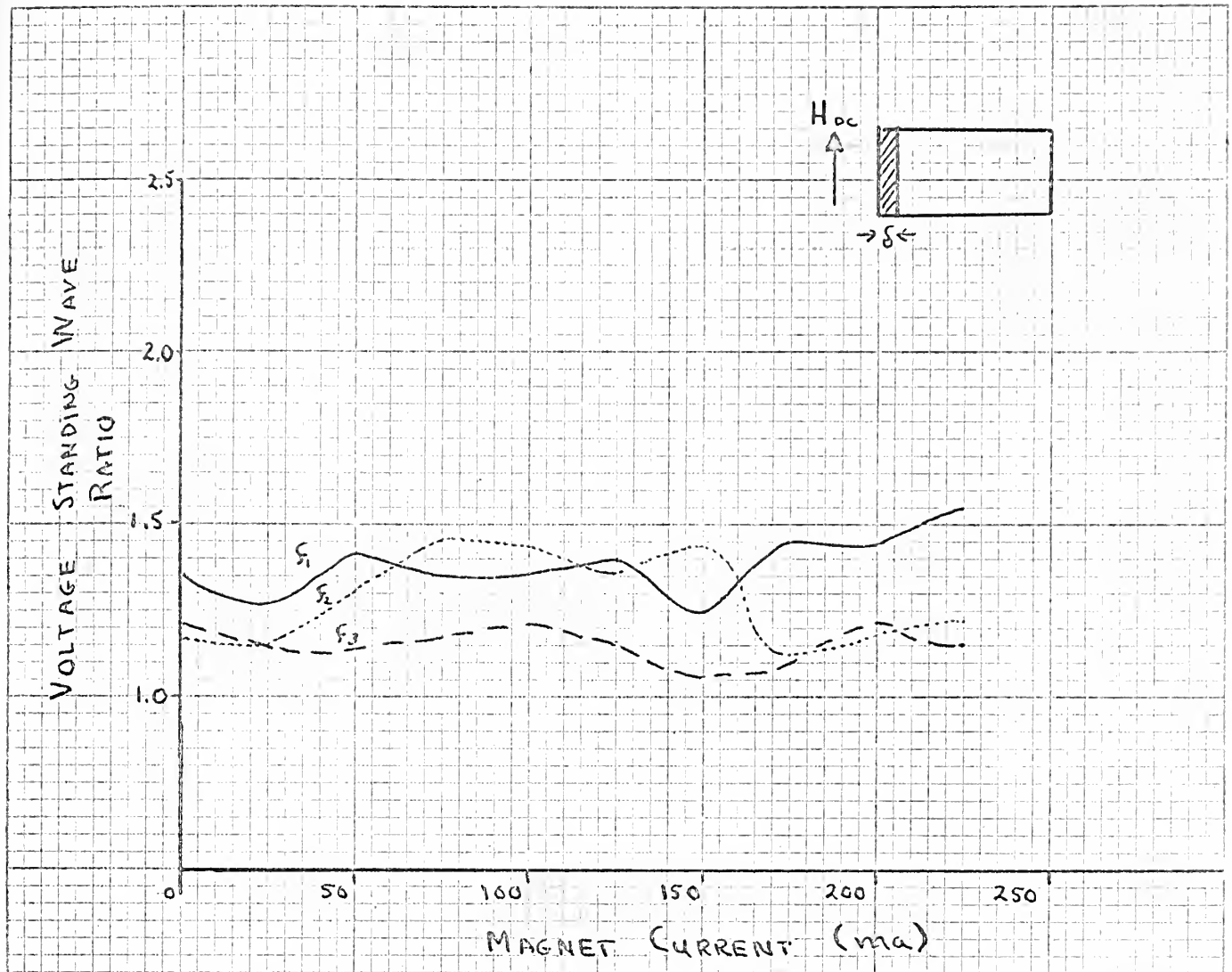

Voltage Standing Wave Ratio vs Magnet Current

Ferrite TT-390
Length L = 5.6" ±0.1"
Thickness δ = 0.0866"
Shape - Rectangular
Frequency - f_1 = 8.97Gc
f_2 = 9.168Gc
f_3 = 9.372Gc

FIG 5-14

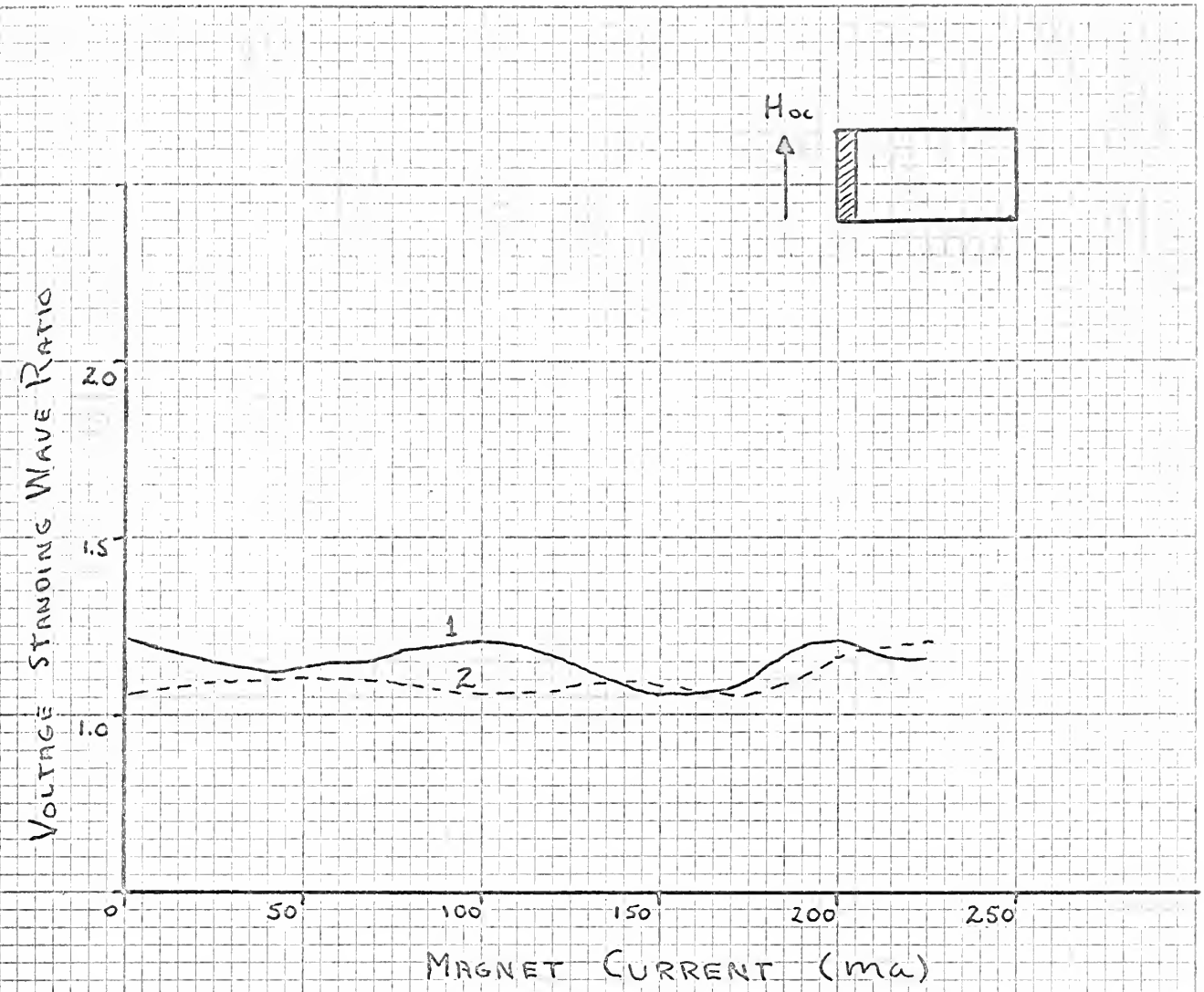

Voltage Standing Wave Ratio vs Magnet Current

Ferrite	TT-390
Length	5.6" ± 0.1"
Thickness	δ = 0.0866"
Frequency	= 9.372 Gc
Shape	1. Rectangular
	2 Ramp taper

FIG. 5-15

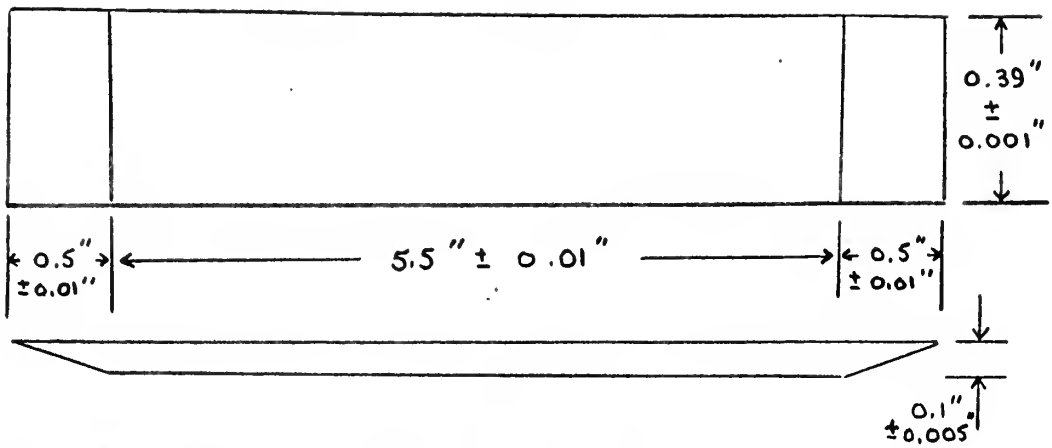

Fig. 5-16 Ferrite Slab for 360° Linear Phase Shift

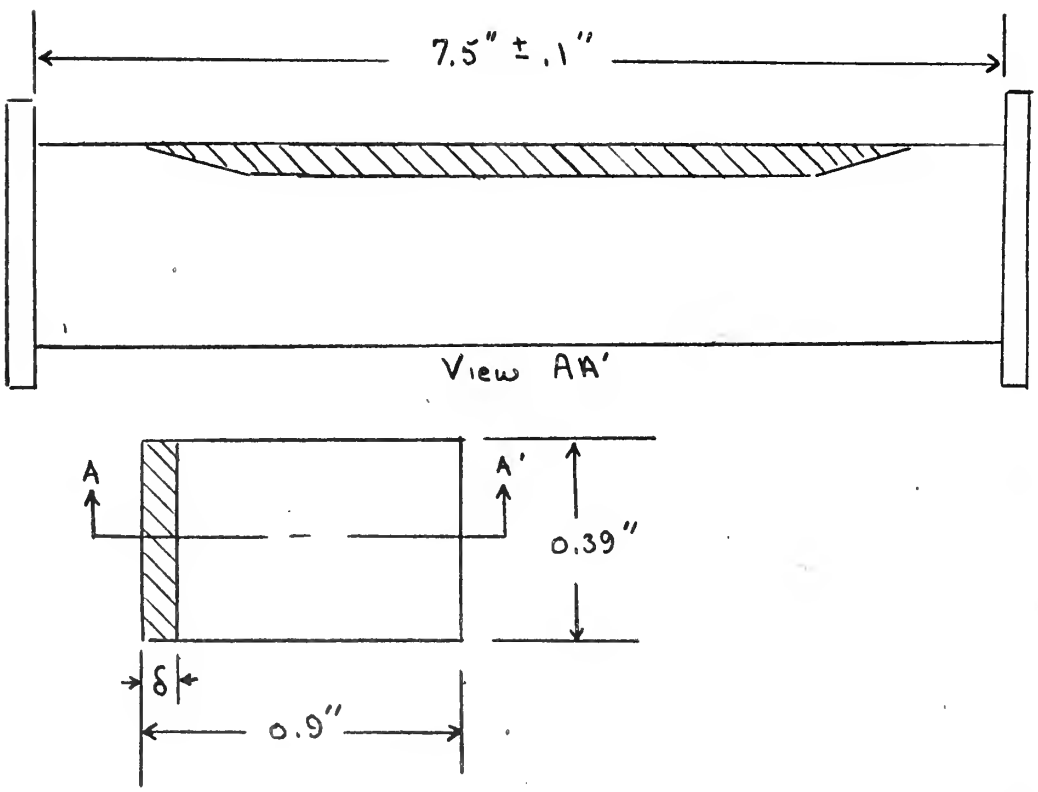

Fig. 5-17 Ferrite Loaded Precision Waveguide Section

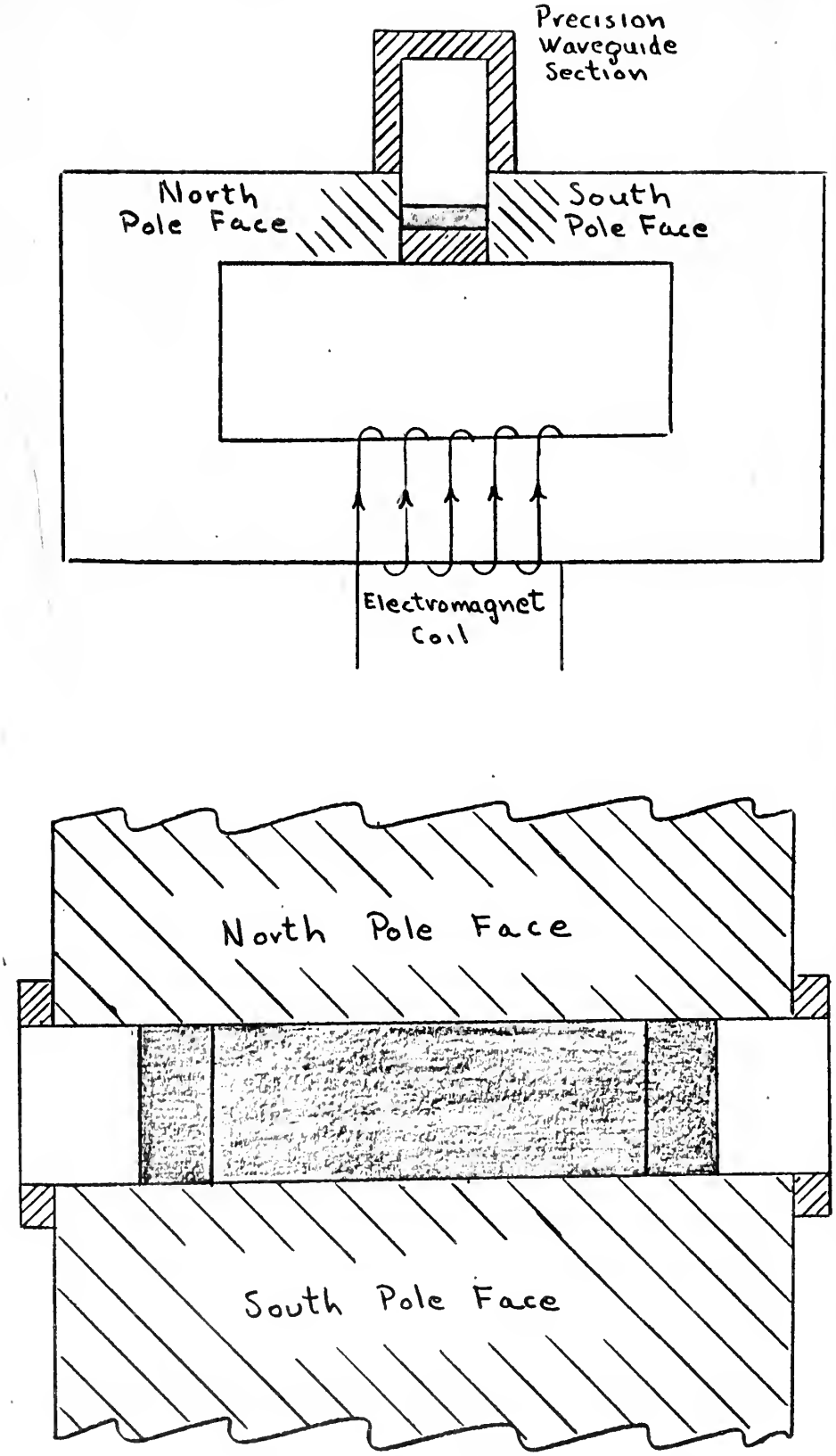

Fig. 5-18 Precision Waveguide with Ferrite and Electromagnet

APPENDIX A

ERROR ANALYSIS

1. Phase Measurement Error

The phase measurement error for the system used in the conduction of experiments with ferrites as the control device are composed of: Insertion Error, Error in the Standard Phase Shifter, Tuning Error, Microscope Error, and Waveguide Width Error. The Total Phase Error is the sum of all of these errors. Each of these errors is discussed in the following paragraphs.

Insertion Error: Assume the SWR of the ferrite device to be 1.5 maximum. As discussed in references (38)and (39), the insertion point is tuned to a null so that the match is as good as the directivity of the directional coupler (assume 40 db). With this assumption the reflection coefficient on either side of the insertion point is approximately 0.01, which gives an SWR of approximately 1.02. The combination of these two SWR's gives a maximum phase error of 0.4 degrees. As the ferrite SWR decreases, so does the phase error (but not in linear relation). For instance, assume insertion point SWR of 1.02 at both sides, then

Ferrite SWR	Maximum Phase Error
1.01	$0.02^{\circ} = 0.03^{\circ}$
1.1	0.08°
1.2	1.15°
1.3	0.2°
1.4	0.3°
1.5	0.4°

Error in Standard Phase Shifter: There are four conditions for computing the error in the standard phase shifter, namely:

a. $\Gamma_{2i} \neq 0$

b. $S_{31} \neq 0$

c. microscope error

d. precision wave guide width tolerance

error. Both Γ_{2i} and S_{31} are tuning errors and are controlled by the tuners shown in figure (A-1).

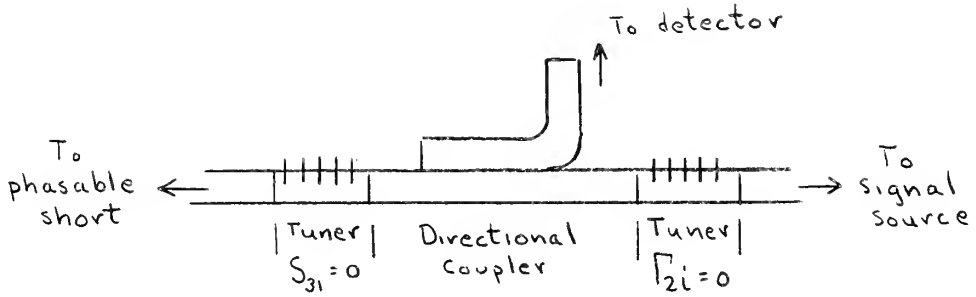

Fig. A-1 Standard Phase Shifter Tuner Controls.

Consider $\Gamma_{2i} \neq 0$ (short circuit tuning). With a variation of $\Delta \Gamma_{2i} \approx 0.01$ db max, then $\left|\Gamma_{2i}\right|$ is 0.00058. The phase error then becomes:

$$\text{Error} = \frac{0.00058 \times 180}{\pi} \left| \sin \frac{\psi_{meas}}{2} \right| \quad \text{(degrees)}$$

$$= 0.033 \left| \sin \frac{\psi_{meas}}{2} \right| \quad \text{(degrees)}$$

ψ (measured angle)	$\psi/2$	$\sin \psi/2$	Phase Error
00	00	0.00	0.0°
90	45	0.707	0.023°
180	90	1.000	0.033°
270	135	0.707	0.023°
360	180	0.00	0.0

Now if $S_{31} \neq 0$ (matched taper tune), but is tuned for $\Delta S_{31} \approx 0.5$ db max using a taper having a return loss of 50db, then

$$\left|S_{31}\right| = 10^{-4}$$

The Phase Error then becomes:

$$\text{ERROR} = \frac{0.0001 \times 180}{\pi} \left| \sin \frac{\psi \text{ meas}}{2} \right| \quad \text{(degrees)}$$

Thus, this error differs from the Γ_{2i} error by $\frac{1}{5.8}$.

ψ (measured)	Phase Error
00°	0.0°
90°	0.004°
180°	0.0058°
270°	0.004°
360°	0.0°

The microscope error is dependent on the scale resolution, which in this case was 50 microinch. This resolution introduced a phase error of 0.04 degrees.

The waveguide width tolerance error depends on the machining tolerance which in this case was 20 microinch. The Phase Error then becomes:

$$\text{Error} = 0.00005 \times \psi \text{ (measured)} \quad \text{(degrees)}$$

ψ (measured)	Phase Error
00°	0.0°
90°	0.0045°
180°	0.0090°
270°	0.0135°
360°	0.0180°
↓	↓
etc	etc

2. Power Measurement Error: The error in measuring the insertion loss change depends entirely on the instrument used in making the

power measurements. In this case an HP 431B was used, introducing and error which was 3% at full scale.

3. SWR Error: Using the modified reflectometer method (55), $\Delta \Gamma_{2i}$ (short circuit tune) is set for approximately 0.01 db and S_{31} (taper tune) using a 50db taper is set for 0.5 db. The VSWR maximum error due to $S_{31} \neq 0$ is approximately 0.06%. The VSWR maximum error due to $\Gamma_{2i} \neq 0$ is:

Ferrite VSWR	VSWR Percent Error
1.5	0.03
1.4	0.022
1.3	0.017
1.2	0.013
1.1	0.006

The total VSWR error is the sum of the two errors.

APPENDIX B

SAMPLE CALCULATIONS

All of the following sample calculations are based on the constants of the ferrite sample as provided by the manufacturer. For the ferrite sample used in the research during the writing of this paper, the following data was provided:

Ferrite sample -- TT-390

Manufacturer -- TRANS-TECH INC., Gaithersburg, Md.

Saturation magnetization ($4\pi M_s$)	2150 gauss
g effective	2.10
Line Width (Δ H)	540
Dielectric Constant	13
Loss tangent	<0.0005
Curie Temperature	320° C

1. Gyromagnetic Ratio.

$\gamma = ge/2mc$

$\gamma = 2.8$ mc/oer, when $g = 2.0$

$\gamma = 2.94$ mc/oer, when $g = 2.1$

2. Field strength for resonance at an operating frequency of 8.97 Gc:

$$H_i = \omega / \gamma$$

$$= 8.97 \times 10^3 / 2.94$$

$$= 3.05 \text{ K gauss}$$

Increasing the operating frequency will require a stronger static field to produce gyromagnetic resonance.

Given any field strength in kilogauss, the gyromagnetic resonant frequency in gigocycle can be computed from:

$$\omega_o = \gamma H_{DC}$$

3. Permeability tensor factors:

Knowing the saturation magnetization ($4\pi M_s$), the operating frequency (ω), and the gyromagnetic resonant frequency (ω_o), the coefficients μ, K and μ_{eff} can be computed from:

$$\mu = 1 + \frac{\gamma 4\pi M_s \omega_o}{\omega_o^2 - \omega^2}$$

$$K = \frac{\gamma 4\pi M_s \omega}{\omega_o^2 - \omega^2}$$

$$\mu_{eff} = \frac{\mu^2 - K^2}{\mu}$$

For the sample used:

$$4\pi M_s \gamma = 2150 \times 2.94 \times 10^6 = 6.32 \times 10^9$$

Computations for various values of H_{DC} are given in table B-1. A plot of μ vs H_{DC} is given in figure (B-1). This plot compares favorable with that presented in figure (2-11) and shows that power absorption commences the field inside the ferrite reaches 2200 gauss. Using reference (54), for the slab sizes used, the external field required to produce the internal field desired is given by:

$$H_{ext} = k_i H_{int}$$

Slab thickness	i	k_i
0.0534	1.	1.16
0.0787	2.	1.16
0.1042	3.	1.22
0.1280	4.	1.23

Table B-1 Calculated values of μ, K and μ_{eff} for various values of internal static field.

H_{DC} Internal	μ	K	μ_{eff}
0250	0.942	-0.707	0.414
0500	0.881	-0.726	0.280
0750	0.816	-0.750	0.130
1000	0.741	-0.791	-0.101
1200	0.672	-(.834	-0.358
1400	0.590	-0.894	-0.765
1600	0.490	-0.974	-1.450
1800	0.362	-1.080	-2.860
2000	0.190	-1.240	-6.210
2100	0.080	-1.330	-22.00
2200	-0.050	-1.460	∤42.60
2300	-0.220	-1.610	∤11.59
2400	-0.470	-1.860	∤ 6.88
2500	-0.750	-2.140	∤ 5.38
2600	-1.160	-2.540	∤ 4.37
2700	-2.860	-4.220	∤ 3.33

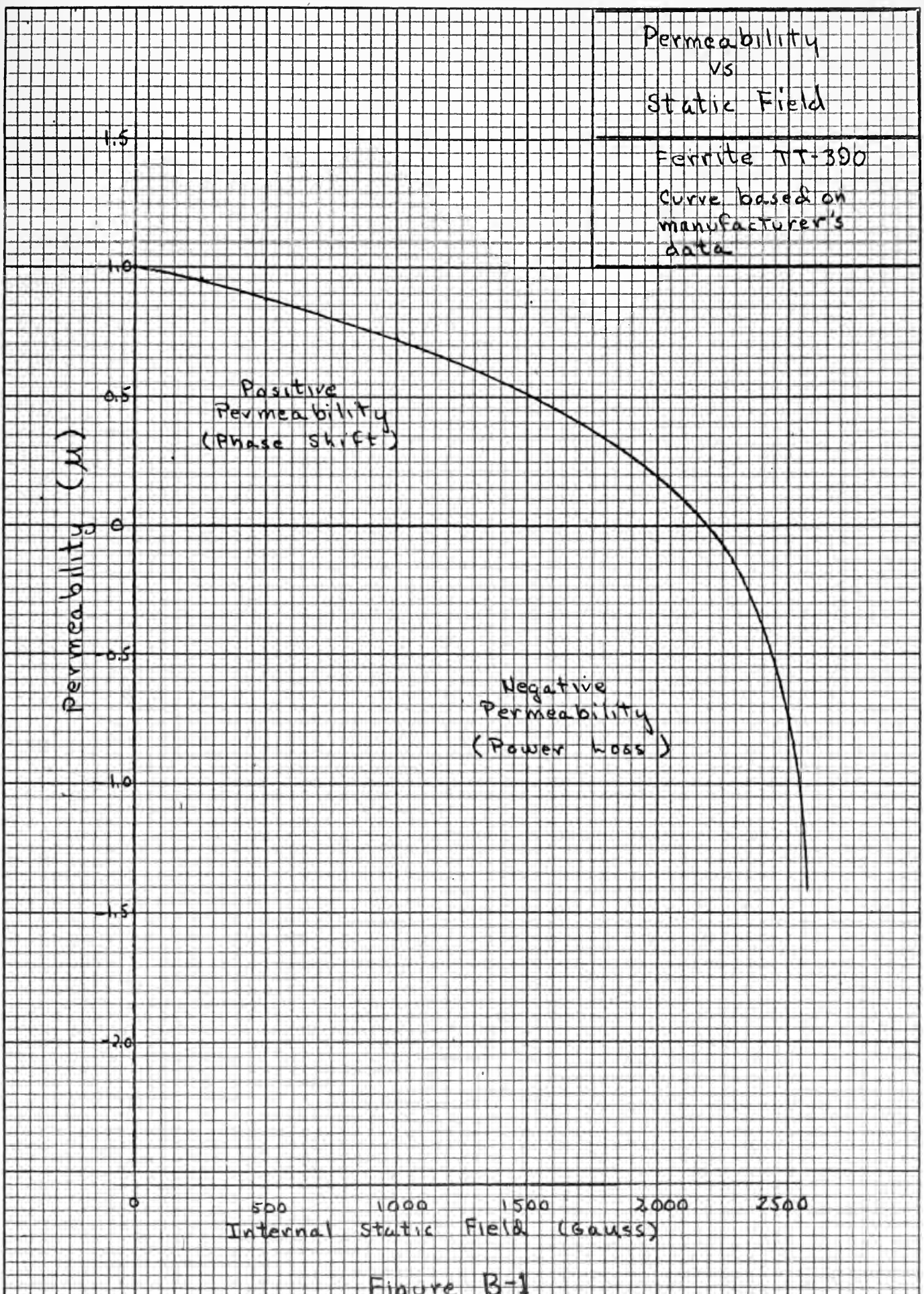
Permeability
vs
Static Field
Ferrite TT-390
Curve based on manufacturer's data
1.5
1.0
0.5
0
-0.5
-1.0
-1.5
-2.0
Permeability (μ)
Positive Permeability (Phase shift)
Negative Permeability (Power Loss)
0
500
1000
1500
2000
2500
Internal Static Field (Gauss)

Figure B-1

BIBLIOGRAPHY

1. A GARDNER FOX, An Adjustable Waveguide Phase Changer, PROC IRE, Dec 47, pp 1489-98
2. C. KITTEL, On the Theory of Ferromagnetic Resonance Absorption, PHYS REV, Vol 73, Jan 48, pp 155-161
3. D. POLDER, On the Quantum Theory of Ferromagnetic Resonance, PHYS REV, Vol 73, May 1948, pp 1116-1120
4. L. NÉEL, Magnetic Properties of Ferrites, Ferrimagnetism and Antiferromagnetism, Annales de Physique (French), Vol 3, p 137, 1948
5. C. L. HOGAN, The Microwave Gyrator, Bell System Tech Journal, Vol 31, 1952, p 1
6. N. G. SAKIOTIS and H. N. CHAIT, Ferrites at Microwaves, PROC IRE, Jan 53, pp 87-93; and Properties of Ferrites in Waveguides, IRE TRANS MTT-1, No 2, Nov 53, pp 11-17
7. J. H. ROWEN, Ferrites in Microwave Applications, Bell System Tech Journal, Vol 32, No 6, Nov 53, pp 1333-1371
8. B. LAX, K. J. BUTTON, and L. M. ROTH, Ferrite Phase Shifters in Rectangular Waveguide, JOUR APP PHYS, Vol 25, Nov 54, pp 1413-1421
9. M. T. WEISS, The Behavior of Ferroxdure at Microwave Frequencies and J. P. VINDING, Microwave Devices Using Ferrite and Transverse Magnetic Field, IRE CONV REC, Part 8, 1955, pp 95-105
10. A. G. FOX, S. E. MILLER, M. T. WEISS, Behavior and Application of Ferrites in the Microwave Region, BSTJ, Vol 34, No 1, Jan 55 pp 5-105

11. E. L. ALDERMAN, Transverse Field Ferrite Phase Shifters in Rectangular Waveguide, Thesis, USN Postgraduate School, 1955

12. C. SIEWART, Some Applications of Ferrite at Wavelengths of 0.87 cm and 1.9 cm, IRE TRANS, MTT-3, Apr 55, No 3, pp 27-31, or IRE CONV REC, 1955, Part 8, p 100

13. E. F. BARNETT, A New Precision X-Band Phase Shifter, IRE TRANS, INSTR, PGI-4, Oct 55, pp 150-154

14. S. WEISBAUM and H. SEIDEL, The Field Displacement Isolator, BSTJ Monograph No 2661, 1956

15. R. F. SOOHOO, Ferrite Microwave Phase Shifters, IRE CONV REC, Part 5, 1956, pp 84-98

16. O. W. FIX, A Balanced Stripline Isolator, IRE CONV REC, Part 5, 1956, pp 99-106

17. K. J. BUTTON and B. LAX, Theory of Ferrites in Rectangular Waveguides, IRE TRANS, PGTAP, AP-4, Jul 56, No 3, pp 531-8

18. P. H. VARTANIAN and E. T. JAYNES, Propogation in Ferrite-Filled Transversly Magnetized Waveguide, IRE TRANS, MTT-4, Jul.56, No 3, pp 140-143

19. FERRITES ISSUE, PROC IRE, Oct 56, with the following specific articles:

    (a) J. H. VAN VLECK, Fundamental Theory of Ferro and Ferri Magnetism, pp 1248-1258

    (b) N. BLOEMBERGEN, Magnetic Resonance in Ferrites, pp 1259-1270

    (c) H. SUHL, The Nonlinear Behavior of Ferrites at High Microwave Signal Level, pp 1270-1284

(d) L. G. VAN UITER, Dielectric Properties of and Conductivity in Ferrites, pp 1294-1303

(e) D. L. FRESH, Methods of Preparation and Crystal Chemistry of Ferrites, pp 1303-1311

(f) C. L. HOGAN, The Elements of Nonreciprocal Microwave Devices, pp 1345-1368

(g) B. LAX, Frequency and Loss Characteristics of Microwave Ferrite Devices, pp 1368-1385

(h) H. SCHARFMAN, Three New Phase Shifters, pp 1456-1459

20. C. D. OWENS, Modern Magnetic Ferrites and Their Engineering Applications, Bell Telephone System Monograph No 2709, 1956

21. W. H. HEWITT, Jr. and W. H. VON AULOCK, A Reciprocal Ferrite Phase Shifter for X-Band, PROC NAT ELEC CONF, Vol 13, Oct 57, pp 459-469

22. F. REGGIA, A New Technique in Ferrite Phase Shifting for Beam Scanning of Microwave Antennas, IRE PROC, Nov 57, pp 1510-1517

23. C. B. SHARPE and D. S. HEIM, A Ferrite Boundary Value Problem in a Rectangular Waveguide, IRE TRANS, MTT-6, Jan 58, No 1, pp 42-46

24. H. A. DROPKIN, Direct Reading Microwave Phase Meter, IRE CONV REC, Part 1, Mar 58, pp 57-63

25. R. R. UNTERBERGER, A Microwave Spin Spectrometer, IRE CONV REC, Part 1, Mar 58, pp 64-72

26. M. E. BRODWIN, Propagation in Ferrite-Filled Microstrip, IRE TRANS, MTT-6, Apr 58, No 2, pp 150-155

27. A. CLAVIN, Reciprocal Ferrite Phase Shifters in Rectangular Waveguides, IRE TRANS, MTT-6, July 58, p 334

28. C. BOWNESS, Microwave Ferrites and Their Applications, Microwave Journal, Vol 1, No 1, Jul-Aug 58, pp 13-21

29. M. MAGID, Precision Microwave Phase Shift Measurements, IRE TRANS, INSTR, PGI-7, Dec 58, pp 321-331

30. E. STERN and R.S. MANGIARACINA, Ferrite High Power Effects In Waveguides, IRE TRANS, MTT-7, Jan 59, No 1, pp 11-15

31. J. L. MELCHOR and P.H. VARTANIAN, Temperature Effects in Microwave Ferrite Devices, IRE TRANS, MTT-7, Jan 59, No 1, pp 15-18

32. D. D. KING, C. M. BARRACK and C. M. JOHNSON, Precise Control of Ferrite Phase Shifters, IRE TRANS, MTT-7, Apr 59, No 2 pp 229-233

33. A. D. BRESLER, On the TE_{no} Modes of a Ferrite Slab Loaded Rectangular Waveguide and the Associated Thermodynamic Paradox, IRE TRANS, MTT-8, No 1, Jan 60, pp 81-96

34. K. J. BUTTON, Historical Sketch of Ferrites and their Microwave Applications, Microwave Journal, Vol 3, No 3, Mar 60, pp 73-79

35. C. A. FINNILA, L. A. ROBERTS and C. SUSKIND, Measurement of Relative Phase Shift at Microwave Frequencies, IRE TRANS, MTT-8, No 2, Mar 60, pp 143-147

36. B. LAX and K.J. BUTTON, Electromagnetic Properties and Their APPLICATIONS from UHF to Millimeter Waves, Part I, Microwave Journal, Vol 3, No 9, Sept 60, pp 43-49 and Part II, Microwave Journal, Vol 3, No 10, Oct 60, pp 52-61

37. G. E. SCHAFER, A Modulated Subcarrier Technique of Measuring Phase Shifts, IRE TRANS INSTR, Vol 1-9, No 2, Sept 1960

38. G. E. SCHAFER and R. W. BEATTY, Error Analysis of a Standard Microwave Phase Shifter, Journal of Research of the National Bureau of Standards, Vol 64 C, No 4, Oct - Dec 1960

39. G. E. SCHAFER, Mismatch Errors in Microwave Phase Shift Measurements, IRE TRANS, MTT-8, No 6, Nov 1960

40. W. J. POLYDOROFF, High Frequency Magnetic Materials, John Wiley & Sons Inc., 1960

41. R. F. SOOHOO, Theory and Application of Ferrites, Prentice-Hall Inc. 1960

42. R. E. COLLIN, Field Theory of Guided Waves, McGraw-Hill Book Co Inc., 1960

43. I. BADY, Ferrites with Planar Anisotropy at Microwave Frequencies, IRE TRANS, MTT-9, No 1, Jan 61, pp 53-62

44. S. S. SANDLER, An Approximate Solution to Some Ferrite Filled Waveguide Problems with Longitudinal Magnetization, IRE TRANS, MTT-9, No 2, Mar 61, pp 162-168

45. R. F. SOOHOO, Theory of Dielectric Loaded and Tapered Field Ferrite Devices, IRE TRANS, MTT-9, No 3, May 61, pp 220-224

46. P. LACY, A Versatile Phase Measurement Method for Transmission Line Networks, IRE TRANS, MTT-9, No 6, Nov 61, p 568

47. W. F. KRUPKE, T. S. HATWICK and M. T. WEISS, Solid State X-Band Power Limiter, IRE TRANS, MTT-9, No 6, Nov 61, pp 472-480

48. P. J. B. CLARRICOATS, Microwave Ferrites, John Wiley & Sons, Inc, 1961

49. R. A. WALDRON, Ferrites (An Introduction for Microwave Engineers), D. Van Nostrand Company Ltd., 1961

50. K. J. STANDLEY, Oxide Magnetic Materials, Oxford at the Clarendon Press, 1962

51. B. LAX and K. J. BUTTON, Microwave Ferrites and Ferrimagnets, McGraw Hill Book Co Inc, 1962

52. R. A. SPARKS, Microwave Phase Measurements, Microwaves, Jan 1963, p 14

53. A. G. GUREVICH, Ferrites at Microwave Frequency, (Translation from Russian), Consultants Bureau Enterprises, 1963

54. P. HLAWICZKA and A. R. MOTRIS, Gyromagnetic Resonance Graphic Design Data, PROC IEE (England), Vol 110, No 4, Apr 63, pp 665-670

55. Standards Laboratory Instrument Calibration Technique, JV-01, VSWR Modified Reflectometers Technique, Metrology Engineering Center, BuWeps Rep, Pomona, Calif.